LANDSCAPE ASSESSMENT OF WEST AND SOUTH TEXAS GRASSLANDS TO INFORM CONSERVATION OF SPOT-TAILED EARLESS LIZARDS IN TEXAS

Final Report 2022
Submitted to the Comptroller's Office of Public Accounts of Texas

Samantha S. Kahl, Blackburn College, 700 College Avenue, Carlinville, Illinois, USA.

***Carlos Portillo-Quintero**, Texas Tech University, College of Agriculture, Department of Natural Resource Management, Lubbock, TX 79409.

Robert Cox, Texas Tech University, College of Agriculture, Department of Natural Resource Management, Lubbock, TX 79409.

Nancy McIntyre, Texas Tech University, College of Arts and Sciences, Department of Biological Sciences, Lubbock, TX 79409.

Gad Perry, Texas Tech University, College of Agriculture, Department of Natural Resource Management, Lubbock, TX 79409.

*****Corresponding PI.

Table of Contents

EXECUTIVE SUMMARY

The Spot-tailed earless lizard (Holbrookia lacerata, STEL) is a species of concern in Texas. This species has specific habitat requirements and has been negatively impacted by habitat modification stemming from human activity over many decades. It is now largely confined to habitat remnants, though its secretive nature and boom-and-bust ecology make studies difficult.

This study used high-resolution remote sensing and field-based to explore potential STEL habitat in fourteen counties: Concho, Crockett, Dimmit, Duval, Irion, Jim Hogg, Kenedy, Kleberg, Midland, Nueces, Runnels, Tom Green, Ward, and Webb. We were successful in achieving our four objectives: A) identify habitat characteristics required for STEL presence; B) map where such habitats can be found in the 14 counties; C) document how relevant habitat characteristics in the historic range of STEL have changed over time; and D) evaluate if buffelgrass invasion poses a threat to STEL.

Field surveys and historical records indicated that suitable STEL habitat is limited to areas with little woody encroachment. Field detections of STEL presence predominantly occurred in counties that contain a mix of agricultural land, bare ground (caliche roads, open grasslands), and native grasslands. Our analyses of remotely sensed data indicated that STEL preferentially inhabit counties characterized by fragmented habitat that is low in woody shrub encroachment. Within counties, STEL locations were characterized by higher percentages of perennial forbs and grasses compared to random matched locations and indicate STEL selection of native grasslands, bare ground, and litter. The latter two categories are increased in croplands. In all cases, the presence of patches of native grassland appears to be essential for STEL presence.

Using very high resolution imagery, we identified such habitat characteristics in roughly one third of the study area. The grassland-dominated class had a total core area of 1,498,896 hectares represented by 3,163,341 patches with a mean area of about 1 ha. The grassland-dominated areas are highly fragmented and dominated by worryingly small patches. Although STEL had historically been found in all 14 study counties, sightings in this study only occurred in three of them: nine in Concho, four in Tom Green, and one in Runnels.

Time series analysis of aerial imagery from 1940’s to 2018 indicated that, across the study area, land cover and land use changes were not dominated by a trajectory. The rate of change varied spatially, with agricultural expansion driving high rates of change from the 1930s to the 1990s in counties such as Nueces and Runnels, but urbanization and industrial development driving land cover and land use changes in the most recent decades. Woody vegetation encroachment increased in some counties (where STEL was not found in the current study) and decreased in others.

Buffelgrass surveys showed the plant much more prevalent in southern than in northern counties where STEL were found. However, the invasive has the potential for further spread and has the potential to significantly reduce STEL habitat in future decades.

Overall, our studies show that habitat disturbance by woody vegetation encroachment and other invasive species could be decreasing the presence of important STEL habitat types and reducing vegetation diversity. At the same time, habitat fragmentation, generally considered negative in conservation studies, has led to an increase in habitat variability in some areas with conditions needed for STEL presence.

High-resolution remote sensing can reliably identify landscape diversity and native grasslands across STEL distribution, informing habitat management and conservation actions for the lizard. In particular, such surveys can create potential habitat maps within the range of the STEL that can be used to inform future surveys, as well as future land management practices for STEL and other native species associated with prairie grasslands.

INTRODUCTION

The grasslands of the Great Plains are one of the most impacted and imperiled biomes in North America, with precipitous declines in native grass cover over the past century due to conversion of native prairies to agricultural and developed forms of land use as well as to the introduction and spread of non-native and invasive grass species, all ultimately affecting wildlife survival (Tilman and Lehman 2001, Giocomo et al. 2017). Such changes are particularly noticeable in agricultural areas as well as in those areas with energy-extraction forms of land use, such as mines, oil pump-jacks and pads, and wind turbines. In Texas, recent expansion of energy-extraction industries has increased land fragmentation (Lopez 2018), reducing the amount of continuous habitat area for many native wildlife species and degrading the remaining prairie remnants. Invasive grasses pose similar habitat degradation issues for many wildlife species by changing the general structure of the landscape. In Texas, for example, buffelgrass (*Pennisetum ciliare*) is one such invasive species that can dominate disturbed prairie remnants (Stohlgren 2006).

Texas wildlife are likely experiencing the negative effects of these forms of habitat degradation and disturbance, though the full extent of these impacts on wildlife remains undefined (Kuvlesky et al. 2002). One species of concern for west and south Texas is the Desert Spot-tailed earless lizard (*Holbrookia lacerata*, STEL), which has a portion of its geographic distribution within Texas. Formerly composed of two subspecies [*H. l. lacerata* and *H. l. subcaudalis*], these were only very recently split into separate species [*H. lacerata* and *H. subcaudalis*]. In our research, we considered the species in the broad sense. Basic ecological information for STEL in Texas has been lacking. STEL have experienced population declines within recent decades and have also exhibited sensitivity to anthropogenic impacts on the environment. Conservation and potential recovery actions for STEL should include assessments of both public and private lands, as per typical ESA recovery measures (USFWS 2011a).

In a 2013 Texas Natural Diversity Database Report by the Texas Parks and Wildlife Department, information was offered about STEL survey and habitat mapping efforts, which included 131 (then) new occurrences, with 9 new observations at historic locations for the species (TPWD 2013). The report also indicated a need for additional surveys and observations for STEL (TPWD 2013). More recently, landscape alterations due to anthropogenic factors throughout Texas were examined, using the STEL as a case study species: Pierre et al. (2018) and Wolaver et al. (2018) assessed landscape-level land use changes from energy production, such as oil platforms, solar panel fields, and turbines for wind energy. As with other forms of land cover change, energy development causes direct habitat loss and possible noise pollution, possible water and soil pollution, and even micro-vibrations in the soil, ultimately causing behavioral changes in STEL. Although these studies indicated some degree of alteration of Texas natural landscapes, information on the actual extent of current unaltered or moderately altered habitat available for STEL had not been assessed.

Population declines in STEL have been attributed to landscape changes that reduce the availability of suitable cover. For example, in the petition to list the STEL as Threatened or Endangered, petitioners stated that land use changes from native land to cropland and grazing land, in addition to associated fencing and development, are serious problems for STEL survival (Wild Earth Guardians 2010, USFWS 2011b). A lack of information about how land cover/land use changes affect STEL is hindering potential conservation recommendations and actions for this species. The petition to list STEL spurred review by the USFWS (Wild Earth Guardians 2010, Ingram 2017). The USFWS ruling on the petition findings stated that the listing of the species may be warranted due to the potential threat from fire ant predation, but that sufficient evidence was not presented for listing of the species at that time for reasons of habitat degradation and decrease in species range (USFWS 2011b). The USFWS subsequently initiated a status review of the species to determine its eligibility for listing (USFWS 2011b, Ingram 2017).

The most recent and updated mapping effort by Texas Parks and Wildlife Department (TPWD) includes the production of a vegetation map for Texas at a geographic scale necessary to understand the distribution of natural vegetation types across the state. The assessment is called the Ecological Mapping System (EMS) and shows the distribution of main vegetation and land use types for the entire state at 10-m pixel resolution. However, the TPWD EMS map does not include impervious surface or any anthropogenic land cover within the general distribution of natural ecosystems (roads, energy developments), which makes the real extent of anthropogenic disturbances difficult to estimate. Given the heterogeneity of Texas landscapes, there is a current need to map vegetation cover at the finest scale possible. It is important for the scientific community to provide a detailed characterization of the species' habitat that can be used for local or regional decision making as well as spatial modeling efforts.

Because of direct habitat loss and fragmentation stemming from landscape conversion, STEL are largely confined to habitat remnants. However, these remnant patches are not pristine because of the presence of invasive species, including buffelgrass. Buffelgrass' native range extends from Africa to Eurasia in drier ecosystems; it has been introduced to Australia and the New World (Williams and Baruch 2000). Buffelgrass is an invasive grass present over much of Texas and is known to alter fire cycles and vegetation structure in the areas that it invades (Daehler and Goergen 2005, Jackson 2005, De la Barrera 2008, Stevens and Fehmi 2009); as such, it could change the habitat and therefore present an obstacle to conservation of STEL and other native grassland species. Documenting the presence of buffelgrass in STEL habitat is, therefore, an additional need for understanding the extent of threats to the species.

The challenge of mapping STEL habitat in a highly heterogeneous landscape

Accurate capture of Earth's increasingly heterogeneous landscapes in the form of land use and land cover (LULC) maps plays a vital role in effective land management and land cover change modeling (Belgiu and Csillik, 2018; Dahdouh-Guebas, 2002; Liu and Yang, 2015; Myint et al., 2011; Skidmore et al., 1997). This heterogeneity is best captured by high-resolution imagery, made available by advancements in remote sensing data acquisition and analysis from airborne and space-borne platforms. High spatial resolution imagery (< 1 m pixel size) provides detailed visualization of objects and individual characterization of targets on the ground with the caveat that these datasets are usually available in small scenes for any location and only available with low spectral depth (~ 4-5 bands). Automated image classification of high spatial resolution scenes has been successfully attempted in case studies using Geographic Object-Based Image Analysis (GEOBIA) methods that integrate spatial (e.g., shape) and textural information in addition to spectral characteristics in remotely sensed images (Belgiu and Csillik, 2018; T. Blaschke, 2010; Yu et al., 2006). Although GEOBIA methods are mostly based on costly commercial software packages, remote sensing communities have nonetheless rendered significant effort to promote the use of object-based methodologies (Blaschke, 2010; Blaschke et al., 2014; Mafanya et al., 2017; Yu et al., 2006). Despite the existence of case studies using GEOBIA on high-resolution imagery, its application on land cover mapping over large land extents is scarce. One limiting aspect is the need to mosaic hundreds of high spatial resolution scenes collected over a broad temporal range, which causes differences between pixel values for the same land cover classes among scenes. This is usually a consequence of differences in illumination among scenes (due to sun angle differences or atmospheric conditions) and/or the season the aerial photography was captured. In this context, traditional parametric and non-parametric pixel-based classification methods often fail to capture the variable characteristics of the landscape because of high intra-class spectral variability, which reduces the statistical separability between classes (Li and Shao, 2014; Yu et al., 2006). In order to perform land cover mapping at large scales (county to national level), it is thus necessary to use efficient methods that allow processing of large quantities of National Agricultural Imagery Program (NAIP) imagery scenes while overcoming the limitations of low spectral resolution and high spectral variability.

The heterogeneous landscapes of central Texas where STEL has been observed are ideal for the application of the GEOBIA approach. These landscapes are characterized by an extensive road network (both paved and unpaved), agricultural land, and urban developments in a matrix of low-biomass grasslands and shrublands. A convenient imagery source for this task is the United States Department of Agriculture (USDA) NAIP, available to users at no cost. NAIP imagery has high spatial resolution (<1 m pixel) and is available for the whole state of Texas for recent years (2016, 2018, 2020). In Texas, the LULC datasets with the highest spatial resolution that are available to the public are the National Land Cover Database (NLCD; Fry et al., 2009; Homer et al., 2011, 2015) and the Texas Parks and Wildlife Department's Ecological Mapping System (EMS) database (Elliott et al., 2014). However, the NLCD and the EMS datasets are only 30-m and 10-m pixel resolution, respectively. Products based on moderate resolution imagery (such as the aforementioned) can be achieved through rapid and efficient supervised classification workflows that offer reasonably accurate estimates of land cover and land use distribution at larger geographic scales. However, when superimposed on higher spatial resolution (e.g., NAIP) orthoimagery, significant discrepancies are evident between datasets regarding boundary, object shape, road alignment, crop layer boundaries, and detection of developed land. Such discrepancies thus limit the use of these data and impose uncertainties in local decision-making that depends on high thematic accuracy.

Because of this, the use of the GEOBIA approach on high spatial resolution imagery is a current need for obtaining accurate habitat information for STEL. The NAIP program in conjunction with the early Texas Orthoimagery Program (TOP) are also able to provide temporal coverage from the mid 1990s until present at periodic rates (2-5 years), which allows assessing contemporary vegetation cover trajectories and make comparisons to early aerial photographs from the 1930s and 1950s.

Research objectives

The objective of our work was to use high resolution remote sensing to quantify the current distribution of STEL habitat in the counties of Concho, Crockett, Dimmit, Duval, Irion, Jim Hogg, Kenedy, Kleberg, Midland, Nueces, Runnels, Tom Green, Ward, and Webb and estimate the rates of vegetation cover change from ~1940s until present for the study area. In addition, we combined our results with other publicly available remote sensing products to better understand STEL habitat conditions and threats. We assessed landscape composition and configuration within the range of STEL in Texas using a two-pronged approach combining remote sensing with field-based ecological surveys used to ground-truth and augment remote imagery. The combination of these two methods allowed us to identify (1) overlapping habitat requirements between *H. lacerata* and *H. subcaudalis*, (2) potential habitat impacts of human development and habitat fragmentation, and (3) effects of invasive species (buffelgrass) on habitat occupancy. This allowed us to address the following research questions: What habitat characteristics are required for STEL? Where are the required habitat characteristics found across the landscapes of west and south Texas? Are habitats with suitable characteristics for these species occupied? How have habitat characteristics changed over time in the historic range of STEL? Does buffelgrass invasion pose a threat to STEL? Does buffelgrass invasion coincide with other land use changes and anthropogenic effects over time?

METHODS

Study area

This study focuses on land cover and land use mapping and intensive field surveys for STEL and buffelgrass presence within the boundaries of Concho, Crockett, Dimmit, Duval, Irion, Jim Hoog, Kenedy, Kleberg, Midland, Nueces, Runnels, Tom Green, Ward, and Webb counties in Texas, USA. Our general study methodology and process (Figure 1) was developed with landscape management applications in mind.

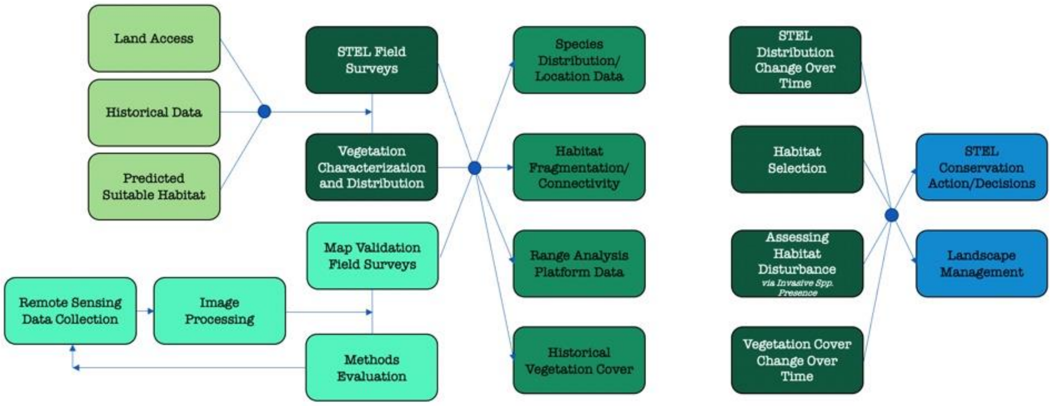

Figure 1. Study methodology and process, with methods and results identified in the process on the left, and how results and inferences can be used to inform applied management (Blue boxes). The cycle on the left also notes the repetitive nature of evaluation following remote sensing data collection and image processing.

TASK 1. Creation of a STEL habitat map using very high resolution imagery

In this study, we used an optimized GEOBIA approach for ingesting, processing, and classifying NAIP imagery into land cover and land use classes over a large area in a time and computationally efficient way. The study processed ~1,500 NAIP scenes for 14 counties in central and South Texas by reducing their spectral dimensionality through principal component analysis (PCA), texture analysis, and edge detection. Objects created through image segmentation were then used to implement a random forest algorithm for classification with minimal post-processing corrections. To our knowledge, our work is the first to attempt a large scale (multi-county) multi-class land use and land cover mapping study using GEOBIA and Machine learning algorithm using only NAIP data.

Our methodology allowed us to discriminate between structural differences in grassland vegetation, specifically to distinguish areas dominated by grass from areas dominated by shrubs or trees (shrublands). In such a classification, grasslands with few scattered trees or shrubs in the landscape are still labeled as grasslands, while areas with higher density of shrubs or trees are labeled in their respective shrubland or forest class. This allows us to clearly identify open grasslands, which are the preferred habitat for STEL. Therefore, our assessment focused on mapping the distribution of the following land cover and land use classes: a) Grassland-dominated land: includes native and non-native grasslands, open areas with short grass and rocky soils (as found in wind turbine sites, oil sites and dirt roads); b) Shrubland-dominated areas: areas with higher density of shrubs and trees and less density of open grasslands; c) Developed land: urban and industrial infrastructure (impervious surfaces) and agricultural land; and d) Waterbodies: lakes and rivers.

1.1 Data Collection

1.1.1 NAIP Imagery

NAIP data have been utilized in several studies using GEOBIA (Baker et al., 2013; Li and Shao, 2014; Maxwell et al., 2019; Nagel and Yuan, 2016) or traditional pixel based classification (Hayes et al., 2014; Knight et al., 2013; Zurqani et al., 2020). The GEOBIA approach yielded higher accuracy in most cases (cf. Hayes et al., 2014).

For this study, we used only NAIP imagery. We acquired ~1,500 Digital Orthophoto Quarter Quads (DOQQs) produced for the period between May 2018 and April 2019. These were acquired from the United States Geologic Survey (USGS) Earth Explorer portal (http://earthexplorer.usgs.gov). Pixel resolution for each scene was 0.6 m. All NAIP imagery DOQQs were downloaded in North American Datum 1983/Universal Transverse Mercator (UTM) Zone 14 North [EPSG:26914]. These DOQQs were mosaicked into a composite band.

1.1.2 Implementation of the GEOBIA Approach

The GEOBIA method is a two-step process that involves transforming a remotely sensed image via 1) image segmentation and 2) classification. We used a GEOBIA approach that starts by mosaicking DOQQs and transforming imagery through principal component analysis (PCA) into uncorrelated bands. PCA can help detect features that are not discernable in the NAIP data while preserving image quality with a reduced number of transformed bands. A texture analysis was applied to PCA products. Texture products (spatial variation of spectral values) characterize the unique degrees of roughness of features or objects present in an image (Franklin et al., 2001). Then a process called Edge Detection was applied to the four NAIP bands, three PCA bands, and the five texture products before segmenting images (Figure 2).

All processes related to this study were accomplished on a Dell Precision M6800 windows workstation computer (64-bit Operating System, Intel® Core™ I7-174940MX CPU @ 3.1 GHz; RAM 32 GB). Spectral indices were also generated from NAIP imagery. These indices are image transformations that are able to quantify pixel level vegetation abundance and moisture content. Aiming at optimizing the processing time and use of computing resources for image segmentation and classification, we split the mosaicked NAIP (i.e., DOQQs), PCA, GLCM, and spectral index layers into smaller sizes (referred to as tiles), with a minimum size of 88.13 km^2 and a maximum of 912.04 km^2 with 150 m overlap on each side. All image tiles were imported to eCognition 9.5 (Trimble, 2020).

Tiled original imagery, PCA bands, and the aggregated edge layer were used as inputs for image segmentation. The process of image segmentation uses the provided information to detect and map groups of pixels (also called "image segments or objects") that have shared shape and spectral characteristics. We used multiresolution segmentation (MRS), spectral difference

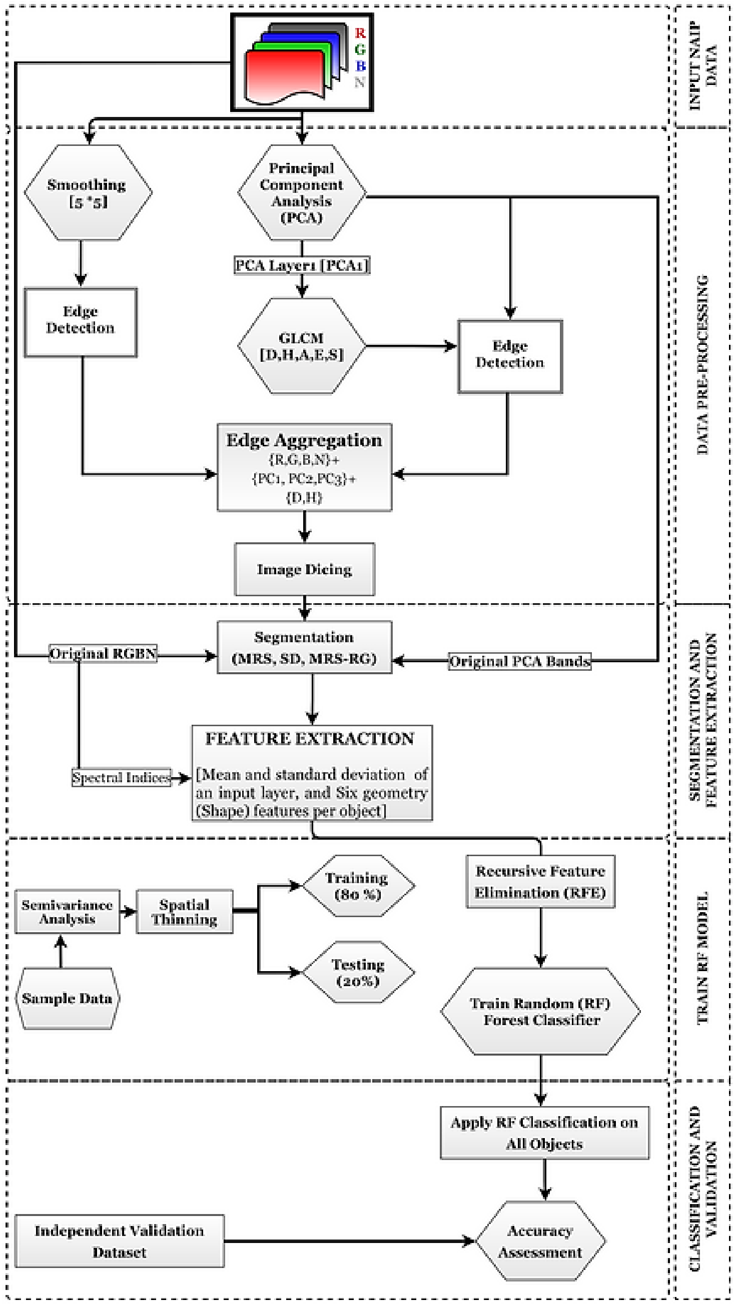

Figure 2. Schematic view of image classification workflow. MRS, SD, and MRS-RG stand for multiresolution segmentation, spectral difference, and multiresolution segmentation region growth, respectively.

segmentation (SDS), and multiresolution segmentation region growth (MRS-RG) techniques on each tile. In Trimble's eCognition software, multiresolution segmentation starts with single pixels as objects and repeatedly merges pairs of objects to form larger objects until local homogeneity remains within a user-specified threshold. In total, 36 variables were calculated on segmented objects (a process also known as feature extraction): mean and stand deviation of four spectral indices, seven geometry (shape) features (asymmetry, compactness, roundness, elliptic fit, rectangular fit, shape index, and density), and mean and standard deviation on four NAIP bands, three PCA bands, and five GLCM textures.

1.1.3 Random Forest model implementation

NAIP-derived segmented objects with values for the 36 variables explained above were then used as input data for a machine learning algorithm (Random Forest) that classified the segmented objects into land cover and land use classes based on input training samples.

1.1.3.1 Model training and testing data

In land use and land cover mapping studies, a usual practice is to split collected training data randomly into training (e.g., 80%) and testing (e.g., 20%). Models are built based on training dataset, and model performance and prediction error are estimated from a testing dataset that was held out from the model-building process. Training datasets were variable among classes and counties, but we applied a rule of thumb of ~200 samples per class per county, which yielded an average of 2,000 training samples per county. However, random selection of observations from a testing data set does not guarantee independence from training observations when spatial dependency is inherent in the data. Therefore, we first created semivariance plots over predictor variables for manually selected samples (training datasets) and determined the maximum distance at which samples were independent (the range distance). Then we applied spatial thinning of samples using the Euclidean distance among sample points to select spatially independent samples (i.e., beyond the range distance).

For the creation of the land cover map, our objective was to map four major land cover classes: active crops, grass-dominated (Grassland), shrub-dominated (Shrubland), and developed/anthropogenic features. During the heads-up on-screen digitization of training sites, we identified two types of features named "Built-up1" (caliche roads or bright features) and "Built-up2" (asphalt roads and different roofs) that represented the developed/anthropogenic class. Agricultural fields that did not have active crops were mapped under the "Fallow land" category. Rivers, lakes, swimming pools, or other water bodies were classified as "water." Due to the high frequency of shadows, we created a separate class for "Shadow" features. Object attributes were extracted for each of the digitized sample points. Finally, the training dataset was split into training (80%) and testing (20%). For model testing, 185 samples were collected for each class based on predicted classes on total objects in the study area.

1.1.3.2 Random forest classification

Before the implementation of the machine-learning algorithm, we applied recursive feature elimination (RFE) to reduce the number of variables to the most important variables. The linear association of a subset of variables (n=34) resulting from RFE was determined using Pearson correlation coefficient (Supplementary Data 1; Figure S1.1). Using the best predictive variables, we used the random forest model on training data with default parameters followed by hyperparameter tuning (splitting parameters and maximum number of trees using a repeated (5 times) 10-fold cross-validation approach. The optimized (with tuned parameters) model was tested based on the highest average producer's, user's, overall accuracy, and Kappa statistics produced on training and testing datasets. We generated the variable importance metric to understand the importance of variables for each class during the decision tree generation process. In a random forest, two measures of importance are given for each class and each variable. The first measure reports the decrease in accuracy when the variable is excluded from the model for classifying out-of-bag (OOB) data (Breiman, 2001). The second measure is based on the decrease of Gini impurity at the splitting node (Breiman, 2001; Breiman et al., 1984). Finally, we classified all objects from all tiles using a random forest (RF) algorithm through the *randomForest* (Liaw and Wiener, 2002) and *caret* (Kuhn, 2020) packages in R 4.0.0 [Figure 3] (R Core Team, 2020).

TASK 2. Habitat validation and map accuracy assessment

2.1 Presence of STEL through field surveys

Field surveys were performed in order to determine locations of STEL in central-west and south Texas counties to identify and classify their local habitat, anthropogenic features, and climate. Our assessments included detection of STEL in relation to the local habitat to determine preferred features and cover on the landscape, and offer insight into the species' behavior with disturbance. We surveyed the 14 counties in Texas as agreed: Ward, Midland, Irion, Tom Green, Runnels, Concho, Crockett, Dimmit, Webb, Duval, Jim Hogg, Kenedy, Nueces, and Kleberg County.

STEL has previously been found in all of the counties surveyed in this research project (Axtell, 1954; Duran and Axtell, 2011; Duran, 2017). Even though STEL is declining, the species is present on some sites where it was previously thought to be extirpated (NatureServe, 2019; Duran and Yandell, 2014; Duran, 2017). STEL was found abundantly in 2015 in counties where it had not been in 50 years (Duran, 2017). This species is considered to have a boom-bust population cycle, booms associated with explosive breeding during very wet years (Axtell, 1954; Duran, 2007). The vegetation and soil profiles differ between the ranges of *H. lacerata* and *H. subcaudalis* (Axtell, 1954, 1956; Duran, 2017). Study sites within known *H. lacerata* range above the Balcones Escarpment contain more juniper/oak woodlands rather than mesquite, and contain less sandy, more clay to non-clay soils (Axtell, 1954, 1956).

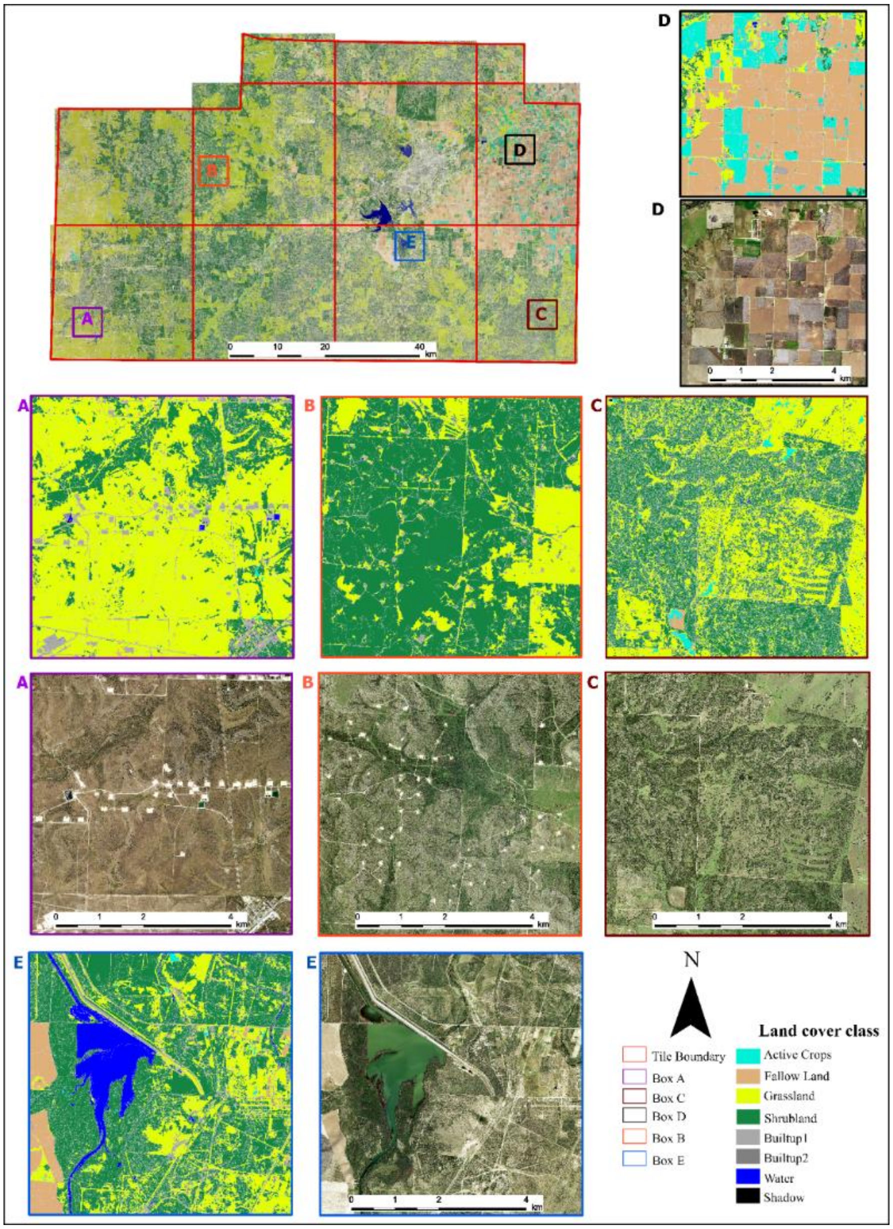

Figure 3: Overview of the land cover classification results for Tom Green and Irion counties using 2018 NAIP imagery. The red grid indicates the extent of a tile without overlap. Subsets of the classified map are displayed as 6 km × 6 km boxes A-E. For each box, a classified map and natural composite NAIP image are displayed with the same letter that also corresponds to the color of the bounding box.

Sites within *H. subcaudalis* range contain more open mesquite woodlands, coastal grasslands, and sandy-clayey loam soils (Axtell, 1954, 1956). Due to the potential rarity of this species, we considered that detection probability tends to be much more variable when targeting less-common lizards (Crump and Forstner, 2019), such as STEL. We explored some more remote possible habitat areas where the species may have been present, though not observed during bust years. We have also documented forms of anthropogenic land use change and potential effects on STEL, building on previously contracted work from other groups (LaDuc et al., 2018).

Road surveys were conducted in areas where spot-tailed earless lizard presence has been recorded in the past, and additional surveys were conducted in areas without historical STEL records. In some counties where public lands were not accessible, areas not preferred by the lizard were also surveyed. In many counties private lands encompassed most of the county and had few public roads, thus, only few road surveys in those counties were conducted. We traveled roads at a slow pace of 10-12 mph, visually scanning the middle of the road, along the road edges, and 5-10 m into the adjacent landscape. If lizards were observed and identified as STEL, we immediately confirmed the lizard's identity visually and recorded the location. We also recorded cloud cover conditions, ranking them from 0 to 4. Cloud cover ranking can be described as follows: 0 = 0% clouds, completely clear skies; 1 = ≤25% clouds, a few clouds; 2 = 25–50%, slightly cloudy; 3 = 50–75% clouds, cloudy; 4 = >75% clouds, overcast. Weather data were retrieved using the National Oceanic and Atmosphere Association (NOAA) database by zip code. We recorded the habitat conditions observed during the survey, and noted potential suitability for observing STEL according to previous work. Suitable habitat conditions have previously been described as areas that are flat, without pure sands or dense woody encroachment, and with some level of disturbance like grazing or agricultural practice (Duran 2017). Unsuitable habitat conditions have been described as areas that aren't flat (sloped or hills present), have pure sands and/or dense woody encroachment and vegetation, and appear to be absent of disturbance (Duran 2017). Opportunistic road surveys in 2020 were conducted on March 18 and again from June 22 through June 26. In 2021, surveys were conducted from the third week of March through the last week of May when spot-tailed earless lizards are most active. Survey minutes were recorded, and we traveled continuously during each survey only stopping to observe STEL and record data.

2.2 Presence of buffelgrass through field surveys

Buffelgrass is native to both tropical and subtropical arid regions of Africa as well as western Asia; however, its exotic distribution spans a much greater area. Outside of its native range, buffelgrass also occupies parts of Australia, the United States, Mexico, and South America (Centre for Arid Zone Research, 2001; United States Department of Agriculture, 2019). This intercontinental spread has been predominantly human-driven (Pauchard and Shea, 2006), with buffelgrass widely introduced around the world as the newest "wonder crop" (Hanselka, 1988). Since its introduction into the United States roughly 100 years ago for forage, it has spread into native vegetation that cannot compete with the drought-tolerant, water-efficient grass. Grice (2006) has even gone so far as to consider buffelgrass a “transformer species,” claiming it has the capacity to change the character, condition, and form of an ecosystem due to its highly competitive nature.

The competitive abilities of this species are becoming apparent in the United States, where buffelgrass was first introduced in 1917 as a trial pasture species. By the 1950s, buffelgrass became commercially available and thrived under the dry conditions (Hanselka, 1988), and by 1985, south Texas ranchers had established buffelgrass on over 4 million hectares of farming land (Cox et al., 1988). It is now spreading (Arriaga et al., 2004) into places such as Arizona, in which it is widely considered a noxious weed (Piggot, 1995). Despite its aggressive nature, however, buffelgrass is still actively planted in pastures as forage for sheep and cattle in south Texas.

The goal of the buffelgrass field survey assessment was to determine how native vegetation, as habitat for the Short-tailed Earless Lizard (STEL), as well as various soil characteristics are affected by the invasion of buffelgrass in Texas. We surveyed the 14 counties in Texas as agreed: Ward, Midland, Irion, Tom Green, Runnels, Concho, Crockett, Dimmit, Webb, Duval, Jim Hogg, Kenedy, Nueces, and Kleberg counties. All counties were surveyed for presence; however, due to the potential lack of buffelgrass presence in the northern Texas counties, the research conducted focused mostly on the counties located in south Texas.

2.3 Map accuracy assessment

In the application of the GEOBIA approach, an average of 2,000 training samples were collected per county based on visual interpretation of the high-resolution imagery. Most of ground-truth information needed to record geographic coordinates of known land cover is satisfied by the high detail in aerial imagery (0.6 m pixel resolution). This pixel resolution allowed us to identify shrublands, developed land, cropland, shadows, and water with high confidence using on-screen digitization. However, the appearance of grasslands in NAIP imagery can be affected by changes in soil moisture in different seasons. Therefore, visual interpretation was aided by field visits in problematic or critical areas that were identified in the mapping process. Roadside inspections of land cover types were necessary in locations across five counties: Irion, Midland, Tom Green, Kleberg and Nueces. Figure 4 shows the extent of systematic roadside inspections made in Irion and Midland counties (Figure 4A and 4D). In Kleberg and Nueces, systematic roadside stops to take GPS measurements were not made in order to avoid possible inquiries by border law enforcement officers. However, observations and fewer stops were made while driving through grassland dominated areas that shown tonality variations in aerial imagery (Figure 4B and 4C). Figure 2E shows an example of the number and spatial spread of final training samples used for image classification. In this example, 2100 samples were used for training and validation of the Tom Green and Irion LULC maps.

We tested the accuracy of the final LULC map using an error or confusion matrix (Congalton, 1991). For generating the validation points, we employed a stratified random sampling with equal allocation strategy using 1480 samples for the counties of Irion and Tom Green.

Reference labels were collected based on field data and fine spatial resolution satellite sensor data available via Google Earth Pro (Tsendbazar et al., 2018). The majority of reference data were labelled from the latter source to offset an access restriction over randomly selected locations, most of which are privately owned. After labelling reference data we calculated a confusion matrix and several accuracy matrices, including user’s and producer’s accuracy (Aronoff, 1982), overall accuracy, Kappa statistic, F1 statistic, and area under the receiver operating curve (ROC). A ROC curve is a standard method of evaluating a presence-absence model (Pontius and Parmentier, 2014). The area under the ROC curve, known as the AUC, has values ranging from 0.5 (random model) to 1.0 (the perfect fit model).

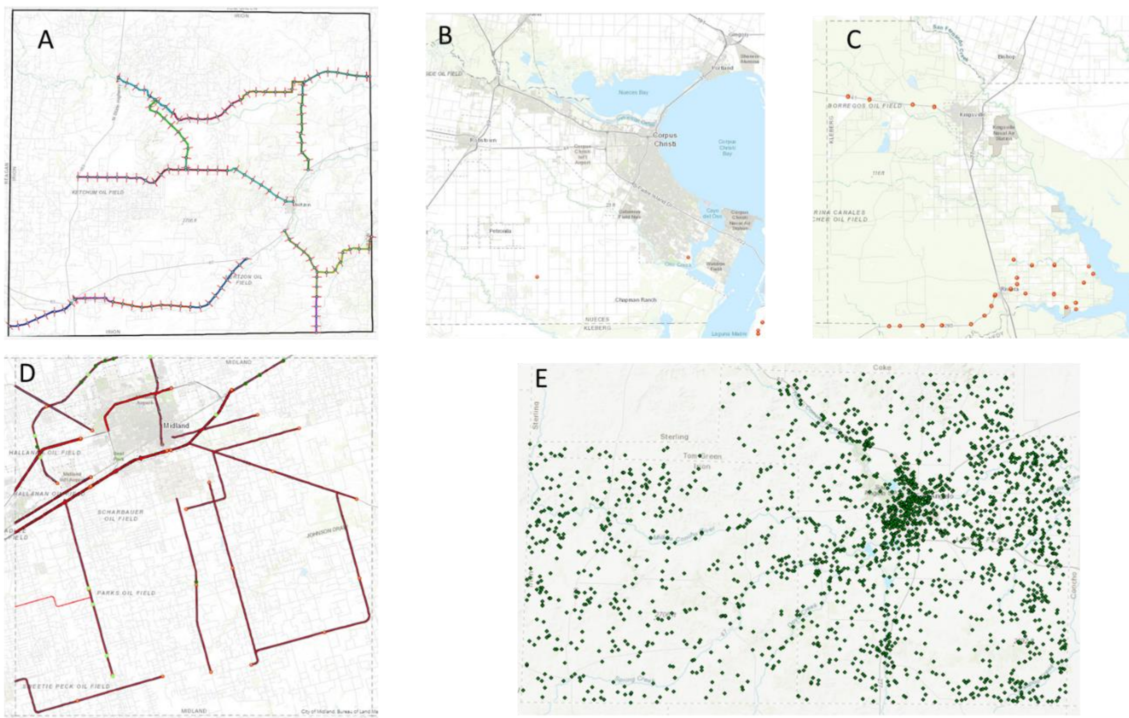

Figure 4. Extent of systematic roadside inspections made in Irion and Midland counties (4A and 4D). In Kenedy and Nueces counties, observations and fewer stops were made while driving through grassland dominated areas in Kenedy and Nueces counties. In these inspections, the cause of observed tonality variations in aerial imagery were validated in the field (4B and 4C). Figure 4E shows 2100 samples that were used for training and validation of the Tom Green and Irion land cover and land use maps through a combination of field visits and high-resolution imagery visual interpretation.

TASK 3. Landscape Metrics and other products.

Landscape-level composition and configuration metrics applied to the generated land cover and land use map allowed us to determine aspects of habitat area, fragmentation, and connectivity for all classes but especially of the grassland-dominated land cover. In order to reduce the data volume and allow the software tools to quantify metrics, we resampled the land cover maps from 0.6 m pixel size to lower resolution pixel sizes (2.5 m, 5 m, 8 m) making sure patch configuration and connectedness remained intact. A 5-m pixel was selected as an appropriate resolution for further landscape fragmentation analysis (Figure 5).

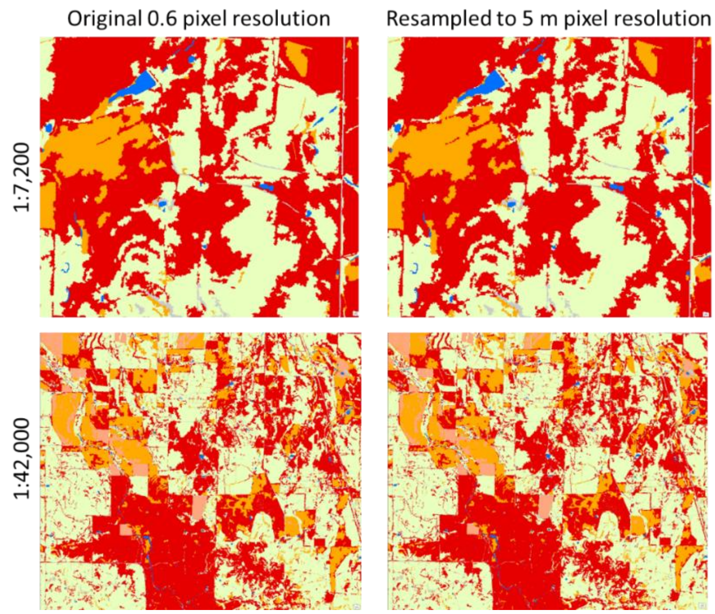

Figure 5. Comparison of the Concho land cover / land use map at 0.6 m pixel resolution and 5 m pixel resolution at two different geographic scales. Resampling the map to 5 m pixel resolution maintains the original patch configuration and extent almost intact, without losing patch interconnectivity.

We used the R package *landscapemetrics* (Hesselbarth, 2019) to quantify eight different class and landscape metrics. This package reimplements the most common metrics from the now-defunct package FRAGSTATS as well as new ones from the current literature on class and landscape metrics. The metrics quantified were:

- Class area (CA): The total (class) area sums the area of all patches belonging to a class. Units are in hectares.

- Proportion of landscape (PLAND): It is the percentage of the landscape belonging to a class. It is a measure of composition and because of the relative character directly comparable among landscapes with different total areas.
- Total Core area (TCA): TCA is a core area metric and equals the sum of core areas of all patches in the landscape. A cell is defined as core area if the cell has no neighbor with a different value than itself (rook's case). In other words, the core area of a patch is all area that is not an edge. It characterizes patch areas and shapes of all patches in the landscape simultaneously (more core area when the patch is large and the shape is rather compact, i.e. a square). Additionally, TCA is a measure for the configuration of the landscape because the sum of edges increase as patches are less aggregated. Units are in hectares.
- Number of patches (NP): NP is an aggregation metric. It describes the fragmentation of a class, however, does not necessarily contain information about the configuration or composition of the class.
- Patch Density (PD): PD is an aggregation metric. It describes the fragmentation of a class, however, does not necessarily contain information about the configuration or composition of the class. In contrast to NP it is standardized to the area and comparisons among landscapes with different total area are possible. Units describe number of patches per hectare.
- Mean Patch area (area_mn): The metric summarizes each class as the mean of all patch areas belonging to class i. The metric is a simple way to describe the composition of the landscape. It can also give an idea of patch structure (e.g., many small patches vs. few larges patches). Units are in hectares.
- Largest patch index (LPI): It is the percentage of the landscape covered by the corresponding largest patch of each class. It is a simple measure of dominance.
- Patch richness (PR): PR is a landscape-level diversity metric. It is one of the simplest diversity and composition measures. It simply measures the number of classes represented by patches in the map.
- Shannon's diversity Index (SHDI): SHDI is a landscape 'Diversity metric'. It is a widely used metric in biodiversity and ecology and takes both the number of classes and the abundance of each class into account. It is unitless.

The equations for each metric can be found in Hesselbarth (2019). Analyses were run for all classes but for practical purposes here, we report results only to describe class-level metrics for the grassland-dominated land cover class with exception of the PR and SHDI indices, which reflect landscape-level configuration using information from all land cover types.

Other products: Percentage of forbs and grasses in grassland-dominated land.

We used a new freely available dataset published by the University of Montana (the Rangeland Analysis Platform; https://rangelands.app/). The RAP datasets provide raster datasets of abundance and distribution of perennial or annual herbaceous, shrubs, trees, and bare ground, and annual aboveground biomass for Western USA at 30-m pixel resolutions from 1986 until 2020. From the 2018 timestep dataset, we combined the “Annual forbs and grasses” and “Perennial forbs and grasses” percentage abundance maps into a single “Annual and perennial forbs and grasses” dataset. This one was subset by the boundaries of grassland-dominated map derived by this project at 0.6 m resolution. By performing this subset, we ensured that RAP observations corresponded to forbs and grass abundance distribution within the available grassland available for STEL.

Other products: Changes in percentages of trees and shrubs from 1986 to 2018.

Using time series data of tree and shrub abundances from the Rangeland analysis Platform, we investigated changes in woody plant abundances from 1986 to 2018. We combined the tree abundance and shrub abundance estimates in order to generate a woody plant abundance map for 1986 and for 2018. We compared the distribution of abundances of woody biomass for both dates and applied an image difference method to generate a map showing the areas with increases or decreases in woody biomass during the last decades within the STEL habitat. We performed this analysis in order to understand the extent of tree and shrub encroachment on STEL habitat and determine potential threats from this ecological process.

Other products: Habitat selection

Using historical records of presence of plateau STEL (*H. l. lacerata*) provided by the Austin Ecological Services Field Office of the US Fish and Wildlife Service, we performed a habitat selection analysis based on vegetation cover data from the Rangeland Analysis Platform. Using ArcGIS, we generated buffers of 200 m radius around all points that intersected our study area. We eliminated overlapping buffer polygons in order to avoid spatial autocorrelation in the data. A total of 49 presence records were used and compared to an identical number of random locations. Using the *adehabitatHS* package in R, we tested whether there were differences between vegetation types and their abundances in areas where STEL had been recorded compared to random sites. The analysis was carried out in two steps: first the significance of habitat selection was tested (using Wilks lambda). Then a ranking matrix was built, indicating whether a given habitat type is significantly used more or less than another habitat type. Manly selection ratios were reported for each land cover type.

TASK 4. Historical vegetation cover change analysis

For assessing historical land cover / land use change in STEL habitat, we initially aimed to compare the distribution of vegetation cover in three times periods: circa 1940s, circa 1986, and circa 2018. The circa 1985 dataset to be used was the TPWD 1984 land cover / land use map for Texas. However, in order to standardize the analysis using the same method across the time series, we used aerial imagery from the Texas Orthoimagery Program (TOP) available circa 1995. Our time series analysis was therefore composed of early aerial photography, TOP imagery from circa 1995, and the 2018 land cover / land use map produced in this study.

The aerial photography acquisition process involved searching the catalog in USGS and Texas Natural Resources Information System (TNRIS) websites (www.earthexplorer.gov, and www.tnris.org). We identified potential data sources [USDA, AMS, TxDOT etc], and dates [>= 1938), and format of data [georeferenced or not]. The best option for this work was the USDA comprised mosaics which already provided large coverage for early dates (1930's and 40's). We proposed to study these changes in several subsets or sample areas of the study area where early aerial photography was available.

Using ArcGIS, we created a grid over the study area with a grid cell resolution of 25 km × 25 km. We used the LCMAP products from 1985 and 2019 to calculate rate of change of scrub (includes grassland and shrub together) for each one of the grid cells. We then categorized grid cells into three classes of land cover change [low, medium, and high] and then selected three grid cells in each category (total 8 grid cells) where early imagery was available. Figure 6 shows the final grid cells selected for further analysis during Spring 2022.

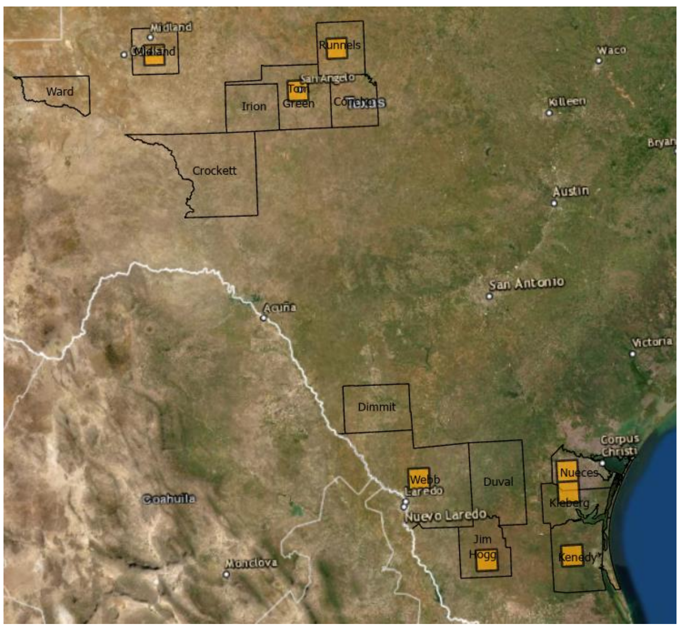

Figure 6. Grid cells selected for the historical land cover / land use change analysis (yellow cells within the Figure) over the 25x25km grid showing grass/shrub changes observed in the LCMAP 1985-2019 products.

At each 25 x 25 km grid cell selected, we applied an image segmentation analysis similar to the process applied to the 2018 NAIP analysis in order to obtain "segments" or "objects" from historical aerial imagery (~1940s) and TOP imagery (~1990s). We then carefully selected all objects corresponding to natural vegetation cover (Figure 7). Vegetation cover includes grassland-dominated areas and shrubland-dominated areas. After digitization of vegetation cover for each time step, we calculated the area in hectares for the vegetation cover class at each time step.

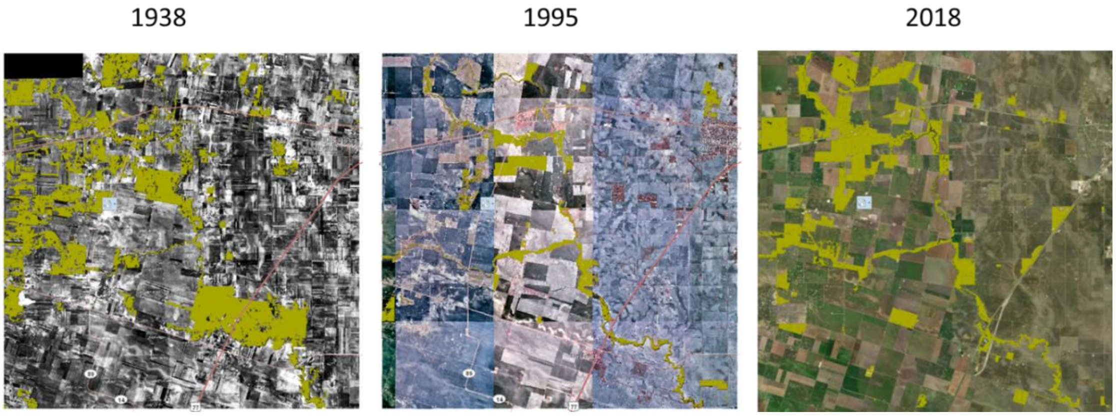

Figure 7. The time series of land cover products from early aerial photographs to more recent NAIP imagery. The mapping process for earlier imagery is aided by the same tools used to derive the 2018 map (image segmentation) although they involve more user visual interpretation.

In Figure 7, we show an example of a 1930's-1995-2018 time series comparison. Using this information, we reported changes in area for each sample and county and calculated the Annual Rate of Change (R) using a standard equation for land cover change from Puyravaud (2003):

$$R = \sqrt[t]{\left(\frac{A}{P}\right)} - 1$$

R = % change
t = time difference
A = Total Amount in Time2
P = Total Amount in Time1

TASK 5. Influence Diagram

We used the information on extent and fragmentation from the STEL habitat map and the information collected from the field (STEL presence, habitat requirements and buffelgrass presence) to build an influence diagram of landscape-scale factors that drive the species management and conservation efforts within the area of interest, with potential applications to other related or similar species with comparable habitat requirements and natural histories.

RESULTS

TASK 1. Creation of a STEL habitat map using very high resolution imagery

The methodology was successfully applied to all counties and maps were uploaded and published for collective visualization using the ArcGIS Online application. The maps will be available for rapid visualization by accessing:

https://www.parktrends.org/stel

Password: stel2021

The datasets have been uploaded to a TechShare drive hosted by TTU Technology Operations and Systems Management (TOSM). Using the TTU "eraider" and password that has been provided, the CPA analyst or IT Department can access the https:\\techshare.ttu.edu website and access the folder named "GST". Within this folder, a sub-folder named "STEL2022-Supplementary Data S2" contains all geospatial products derived by this project along with its corresponding metadata.

Both the website and the TechShare data folder provide access to county-scale maps and a map showing 14 counties together (Figure 8). Table 1 shows basic statistics of land cover and land use proportions and extent by county. Results indicate that the grassland-dominated area extends for 1,958,247 hectares (which corresponds to roughly 12,583 square kilometers). More in-depth discussion on the distribution and configuration of grassland-dominated areas follows under the section on landscape structure analysis (Task 3).

TASK 2. Habitat validation and map accuracy assessment

2.1 Presence of STEL through field surveys

A total of 43 surveys were conducted to identify STEL distribution and habitat in Central and South Texas (Figure 9; Supplemental Data S1: Table S1.1 and Table S1.2). No lizards were observed in Duval, Webb, Jim Hogg, Kleberg, Nueces and Dimmit counties. Though STEL was only observed in counties where historical localities already exist, more survey hours (compared to previous studies) were spent searching for STEL in those counties where STEL were not found, to ensure lack of confirmation bias. In terms of behavior, we did observe STEL at temperatures below what is noted in the current literature, and in inclement weather conditions. This suggests that past surveys may have used search parameters that were too narrow.

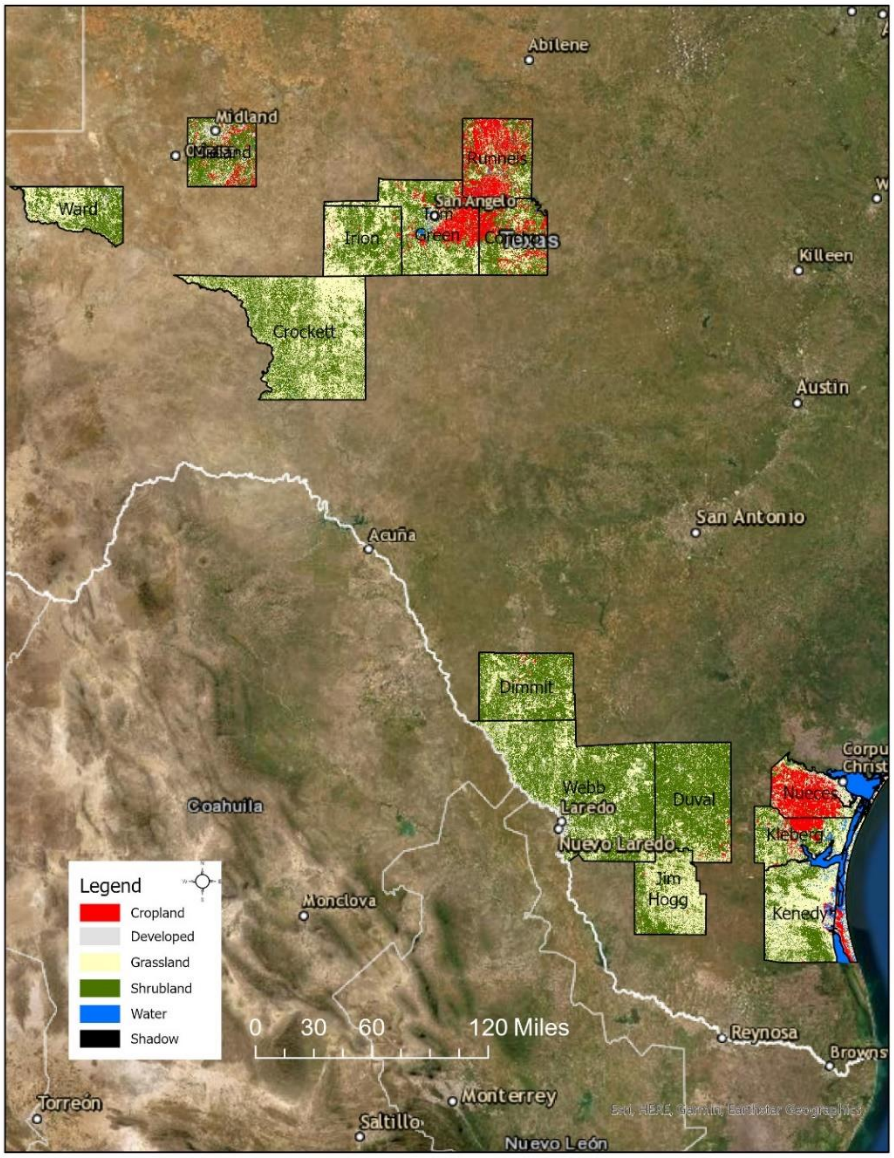

Figure 8. Final land cover map at 0.6 m pixel resolution derived from NAIP imagery analysis for 14 counties within the STEL distribution.

Figure 9. STEL perching on vegetation. Photo by C. Jacobi, 2021.

Table 1. Extent (in square kilometers) of all mapped land cover classes as observed in very high resolution NAIP imagery. The "Shadow" class corresponds to unidentified land cover in dark pixels in shadowed areas. The green-shaded column indicates the primary habitat type for STEL.

	Land Use Land Cover Type (Sq.km)							Total Area (sq.km)
County	Active Crops	Fallow Land	Grass Dominated	Shrub Dominated	Developed	Water	Shadow	
Crockett	0	1	3819	3304	125	19	6	7275
Webb	1	9	2868	5383	417	35	17	8730
Kenedy	6	191	2308	1297	207	574	25	4608
JimHogg	14	14	1644	1220	47	1	0	2940
Tom Green	172	603	1415	1586	156	42	13	3989
Irion	14	37	1257	1333	80	3	1	2725
Dimmit	15	43	1053	2217	72	10	3	3412
Kleberg	16	343	1028	798	35	384	10	2614
Duval	34	29	969	3494	110	3	8	4646
Ward	1	4	934	1094	126	3	3	2165
Concho	425	165	766	1147	32	33	2	2571
Runnels	822	375	601	788	98	44	8	2736
Nueces	63	1149	551	180	237	642	12	2833
Midland	324	33	368	1295	302	8	8	2339

Southern Counties of Duval. Webb, Jim Hogg, Kleberg, Kenedy, Nueces, and Dimmit

A total of 1262.00 survey minutes in 15 surveys were performed in the southern seven counties of the study region. The average highest daily air temperature during surveys was 31.5°C (SD = 3.15°C). Weather conditions overall in Southern Counties were moderately favorable for detection of STEL with most (10/15) surveys conducted during clear or mostly clear sky days. Approximately 30% of surveys were conducted in areas with surrounding habitat that is favorable for detecting STEL, however STEL was not detected during any survey in these southern seven counties (Table S1.1).

Central Counties of Tom Green, Runnels, Crocket, Concho, Irion, Midland, and Ward

A total of 28 surveys were perfomed with a total of 1773 survey minutes in the central seven counties of the study region. The average amount of survey minutes per survey was 63.32 minutes (SD = 34.7 minutes). The average highest daily air temperature was 32.07°C (SD = 3.4°C). STEL was observed in a variety of weather conditions. Half (11/22) of STEL observations were during weather conditions that are not traditionally favorable for detecting STEL, however, 82% (23/28) of surveys were conducted during clear or mostly clear skies, and in areas with surrounding habitat of agricultural fields or grazed rangelands that are favorable for detecting STEL. Twenty two STEL were observed (Table S1.2). When only considering the surveys when STEL was found, the number of lizards found per survey minute was 1 per 20.8 minutes. The highest rate of STEL found per minute during a single survey was 1 per 7.5 minutes, located in Tom Green County when weather conditions and surrounding habitat was favorable for detecting STEL. During field surveys, STEL was observed on or near caliche roads in predominantly agricultural areas in the counties of Concho, Runnels and Tom Green. In the first field survey campaign, no STEL presence was observed. It is important to note that in these first campaigns, the majority of the land cover surveyed was “wooded rangelands.” In the second campaign, the majority of sites were caliche roads in proximity of agricultural areas.

2.2 Presence of buffelgrass through field surveys

We surveyed all 14 counties for buffelgrass presence. Table 2 displays the presence or absence of buffelgrass within those counties. In the process of surveying the 14 target counties, we confirmed buffelgrass presence in the following counties: Bee, Bexar, Brewster, Brooks, Frio, Hidalgo, Jim Wells, Maverick, Medina, Starr, Zapata, and Zavala. Likewise, we attempted but did not observe buffelgrass in the following counties as part of this or other research: Atascosa, Bastrop, Brazos, Brewster, Burleson, Caldwell, Cameron, Culberson, Edwards, Falls, Guadalupe, Hudspeth, Jeff Davis, Karnes, Kerr, Kimble, Kinney, Lee, Live Oak, Loving, McLennan, Menard, Presidio, Real, Refugio, Reeves, Robertson, San Patricio, Uvalde, Val Verde, Victoria, Willacy, Wilson, and Winkler.

Table 2. Counties surveyed as of 03/2022 for buffelgrass presence.

County	Status	Present in Bordering County?
Concho	Not Present	No: Runnels, Tom Green
Crockett	Not Present	No: Irion, Val Verde
Dimmitt	Present	Yes: Maverick, Zavala, Frio, Webb, La Salle
Duval	Present	Yes: Webb, McMullen, Jim Wells, Brooks; No: Jim Hogg
Irion	Not Present	No: Tom Green
Jim Hogg	Not Present	Yes: Webb, Duval, Brooks, Starr, Zapata
Kenedy	Present	Yes: Kleberg, Brooks; No: Willacy
Kleberg	Present	Yes: Kenedy, Brooks, Jim Wells, Nueces
Midland	Not Present	No bordering counties surveyed
Nueces	Present	Yes: Kleberg, Jim Wells; No: San Patricio
Runnels	Not Present	No: Concho, Tom Green
Tom Green	Not Present	No: Irion
Ward	Not Present	No: Loving, Winkler, Reeves
Webb	Present	Yes: Dimmit, Duval, Zapata, La Salle; No: Jim Hogg

2.3 Map validation and accuracy assessment

We tested the land cover and land use map accuracy using fine-scale data from Irion and Tom Green counties. The overall accuracy was 94.80% and a Kappa statistic of 94.10% was achieved (Table 3; Supplementary Data 1; Table S1.3). All eight classes had user's accuracy of >85% and producer's accuracy of >90%. Fallow land, Built-up2, and Shrubland features were better discriminated with the highest F1-scores. These findings suggest very satisfactory performance of the mapping process.

The predictive performance of the RF model based on the receiver operating characteristic curve and the area under the ROC curve indicates superior performance of RF model in discriminating candidate classes. The random forest model yielded more than 95% of the area under the ROC curves for all eight classes, suggesting the model's performance was excellent (cf. Lobo et al., 2008). The highest area was obtained for Shadow and Built-up1, and the least area was obtained for Active crops.

Vegetation and water/moisture indices (NDVI, MSAVI, and NDWI) were among the most important variables for mapping all eight classes based on a mean decrease in accuracy and Gini (Supplementary Data, Figure S1.2). Furthermore, the mean of three principal component bands (MPC1, MPC2, and MPC3), along with the mean of four original bands of the NAIP imagery (MBLU, MGRN, MRED, and MNIR), were among the top 10 variables identified.

Table 3. The error matrix for RF classification using 34 variables from 1480 validation objects selected based stratified random sampling with equal allocation (an error matrix with cell frequency/area is presented in Table S1.1).

LULC Class	Accuracy		Specificity†	F1-score[@]
	User's (Precision)	Producer's (Recall)		
Active Crops	89.19%	91.16%	99.13%	90.16%
Fallow land	97.84%	95.77%	99.69%	96.79%
Grassland	96.22%	91.75%	99.46%	93.93%
Shrubland	98.38%	93.81%	99.77%	96.04%
Built-up1	92.43%	99.42%	98.93%	95.80%
Built-up2	97.84%	95.26%	99.69%	96.53%
Water	93.51%	96.11%	99.08%	94.79%
Shadow	92.97%	95.56%	99.00%	94.25%
Overall Accuracy	94.80%			
Kappa	94.10%			

†Specificity indicates the correct prediction of negative values.
[@]F1-Score is the harmonic mean of precision and recall.

TASK 3. Quantitative description of landscape structure

County-by-county patterns

For comparative purposes, Figure S1.3 and Figure S1.4 (Supplementary Data S1) show the nine landscape metrics results for each county. Counties are organized alphabetically.

- **Kenedy**: In this county, the grassland-dominated area extends for 230,828 hectares, which represents 41% of the county (PLAND). The grassland-dominated class has a total core area of 186,390 hectares (80% of its extent). The class is represented by 294,379 patches (NP), a patch density of 53 patches per hectare with a mean area of 0.8 ha. The largest patch occupies 13% of its extent (LPI). All classes are present in the county (PR=10). The Shannon's diversity index for this county was 1.59, which represents the 64th percentile of the SHDI of all counties. This indicates that the balance between the number of land cover classes and their proportions in the county is above the average.

- **Kleberg**: In this county, the grassland-dominated area extends for 102,817 hectares which represents 25% of the county (PLAND). The grassland-dominated class has a total core area of 87,213 hectares (84% of its extent). The class is represented by 45,963 patches (NP), a patch density of 13 patches per hectare with a mean area of 2.2 ha. The largest patch occupies 6% of its extent (LPI). All classes are present in the county (PR=10). The Shannon's diversity index for this county was 1.65, which represents the 79th percentile of the SHDI of all counties. This indicates that the balance between the number of land cover classes and their proportions in the county is above the average, in the upper quarter of the distribution.
- **Nueces**: In this county, the grassland-dominated area extends for 55,081 hectares which represents 12% of the county (PLAND). The grassland-dominated class has a total core area of 40,581 hectares (73% of its extent). The class is represented by 81,274 patches (NP), a patch density of 18 patches per hectare with a mean area of 0.7 ha. The largest patch occupies 1% of its extent (LPI). All classes are present in the county (PR=10). The Shannon's diversity index for this county was 1.76, which represents the 93rd percentile of the SHDI of all counties. This indicates that the balance between the number of land cover classes and their proportions in the county is above average, in the upper quarter of the distribution.
- **Jim Hogg**: In this county, the grassland-dominated area extends for 164,421 hectares which represents 48% of the county (PLAND). The grassland-dominated class has a total core area of 135,670 hectares (82% of its extent). The class is represented by 84,015 patches (NP), a patch density of 25 patches per hectare with a mean area of 2 ha. The largest patch occupies 18% of its extent (LPI). All classes are present in the county (PR=10). The Shannon's diversity index for this county was 1.15, which represents the 21th percentile of the SHDI of all counties. This indicates that the balance between the number of land cover classes and their proportions in the county is below the average, in the lower quarter of the distribution.
- **Duval**: In this county, the grassland-dominated area extends for 96,905 hectares which represents 19% of the county (PLAND). The grassland-dominated class has a total core area of 66,222 hectares (68% of its extent). The class is represented by 26,1917 patches (NP), a patch density of 52 patches per hectare with a mean area of 0.4 ha. The largest patch occupies 2% of its extent (LPI). All classes are present in the county (PR=10). The Shannon's diversity index for this county was 0.99, which represents the <1 percentile of the SHDI of all counties. This indicates that the balance between the number of land cover classes and their proportions in the county is in the top bottom of the distribution.
- **Webb**: In this county, the grassland-dominated area extends for 286,838 hectares which represents 19% of the county (PLAND). The grassland-dominated class has a total core area of 193,833 hectares (67% of its extent). The class is represented by 1,164,740 patches (NP), a patch density of 79 patches per hectare with a mean area of 0.2 ha. The largest patch occupies 2% of its extent (LPI). All classes are present in the county (PR=10). The Shannon's diversity index for this county was 1.25, which represents the 36th percentile of the SHDI of all counties. This indicates that the balance between the number of land cover classes and their proportions in the county is below the average.

- **Dimmit**: In this county, the grassland-dominated area extends for 105,255 hectares which represents 29% of the county (PLAND). The grassland-dominated class has a total core area of 78,075 hectares (74% of its extent). The class is represented by 215.769 patches (NP), a patch density of 60 patches per hectare with a mean area of 0.5 ha. The largest patch occupies 7% of its extent (LPI). All classes are present in the county (PR=10). The Shannon's diversity index for this county was 1.04, which represents the 7th percentile of the SHDI of all counties. This indicates that the balance between the number of land cover classes and their proportions in the county is below average, in the lower quarter of the distribution.
- **Crockett**: In this county, the grassland-dominated area extends for 381,949 hectares which represents 25% of the county (PLAND). The grassland-dominated class has a total core area of 287,212 hectares (75% of its extent). The class is represented by 526,200 patches (NP), a patch density of 34 patches per hectare with a mean area of 0.7 ha. The largest patch occupies 9% of its extent (LPI). Almost all classes are present in the county (PR=9). The Shannon's diversity index for this county was 1.07, which represents the 14th percentile of the SHDI of all counties. This indicates that the balance between the number of land cover classes and their proportions in the county is below the average, in the lower quarter of the distribution.
- **Irion**: In this county, the grassland-dominated area extends for 125,731 hectares which represents 42% of the county (PLAND). The grassland-dominated class has a total core area of 107,808 hectares (85% of its extent). The class is represented by 74,857 patches (NP), a patch density of 25 patches per hectare with a mean area of 1.7 ha. The largest patch occupies 8% of its extent (LPI). All classes are present in the county (PR=10). The Shannon's diversity index for this county was 1.19, which represents the 29th percentile of the SHDI of all counties. This indicates that the balance between the number of land cover classes and their proportions in the county is below the average.
- **Tom Green**: In this county, the grassland-dominated area extends for 141,502 hectares which represents 17% of the county (PLAND). The grassland-dominated class has a total core area of 109,108 hectares (77% of its extent). The class is represented by 129,675 patches (NP), a patch density of 16 patches per hectare with a mean area of 1.1 ha. The largest patch occupies 3% of its extent (LPI). All classes are present in the county (PR=10). The Shannon's diversity index for this county was 1.41, which represents the 50th percentile of the SHDI of all counties. This indicates that the balance between the number of land cover classes and their proportions in the county is in the middle of the relative distribution among counties.
- **Concho**: In this county, the grassland-dominated area extends for 76,600 hectares which represents 27% of the county (PLAND). The grassland-dominated class has a total core area of 59,582 hectares (77% of its extent). The class is represented by 45,924 patches (NP), a patch density of 16 patches per hectare with a mean area of 1.7 ha. The largest patch occupies 1% of its extent (LPI). All classes are present in the county (PR=10). The Shannon's diversity index for this county was 1.54, which represents the 59th percentile of the SHDI of all counties. This indicates that the balance between the number of land cover classes and their proportions in the county is above the average.

- **Runnels**: In this county, the grassland-dominated area extends for 60,057 hectares which represents 21% of the county (PLAND). The grassland-dominated class has a total core area of 44,474 hectares (74% of its extent). The class is represented by 69,250 patches (NP), a patch density of 24 patches per hectare with a mean area of 0.9 ha. The largest patch occupies 2% of its extent (LPI). All classes are present in the county (PR=10). The Shannon's diversity index for this county was 1.72, which represents the 86th percentile of the SHDI of all counties. This indicates that the balance between the number of land cover classes and their proportions in the county is above the average, in the upper quarter of the distribution.
- **Ward**: In this county, the grassland-dominated area extends for 93,416 hectares which represents 25% of the county (PLAND). The grassland-dominated class has a total core area of 77,920 hectares (83% of its extent). The class is represented by 80,237 patches (NP), a patch density of 21 patches per hectare with a mean area of 1.2 ha. The largest patch occupies 6% of its extent (LPI). All classes are present in the county (PR=10). The Shannon's diversity index for this county was 1.33, which represents the 43rd percentile of the SHDI of all counties. This indicates that the balance between the number of land cover classes and their proportions in the county is below the average.
- **Midland**: In this county, the grassland-dominated area extends for 36,849 hectares which represents 13% of the county (PLAND). The grassland-dominated class has a total core area of 24,807 hectares (67% of its extent). The class is represented by 89,141 patches (NP), a patch density of 32 patches per hectare with a mean area of 0.4 ha. The largest patch occupies <1% of its extent (LPI). All classes are present in the county (PR=10). The Shannon's diversity index for this county was 1.61, which represents the 71st percentile of the SHDI of all counties. This indicates that the balance between the number of land cover classes and their proportions in the county is above the average.

To summarize these patterns, we created a scatter plot of two landscape metrics: a) the LPI as an indicator of grassland dominance and continuous coverage at the county scale and b) the SHDI as an indicator of class diversity or landscape heterogeneity (Figure 10). We use patterns observed in this scatter plot to discuss general trends in the landscape compared to STEL historical presence (see Discussion).

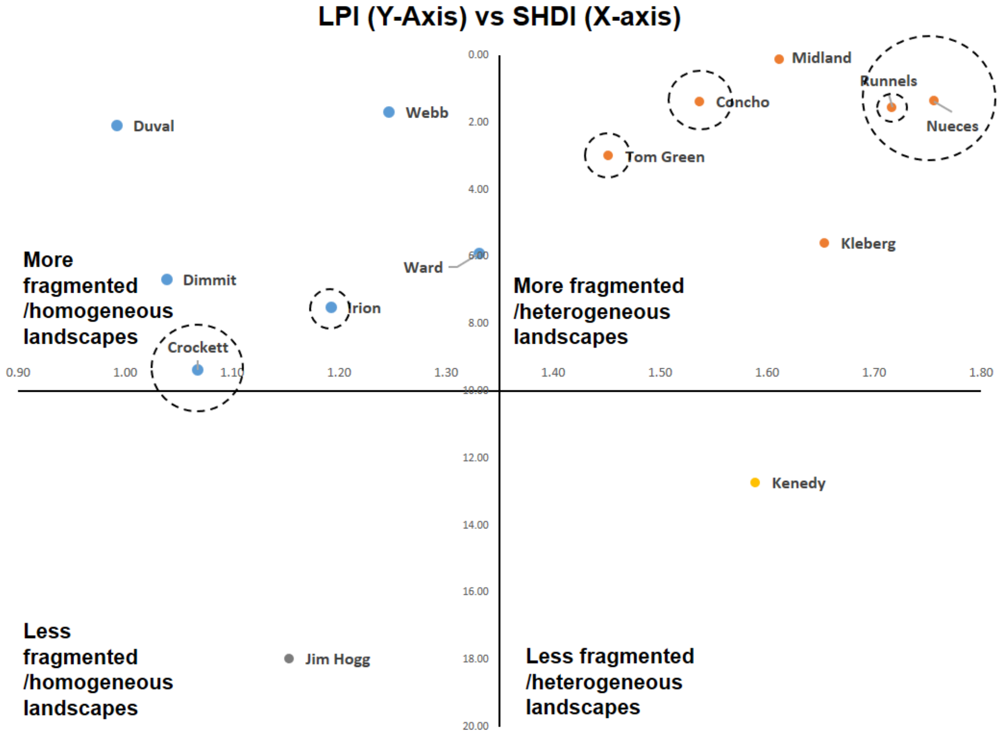

Figure 10. Scatterplot based on the Largest Patch Index (LPI) [Y-Axis] and landscape Shannon's Diversity Index (SHDI) values [X-axis] for all counties. The combination of indices allows us to identify areas with different degrees of grassland fragmentation and landscape-scale diversity. Circles represent relative magnitude (number) of field observations based on historical records for *H. lacerata* and *H. subcaudalis* (2008-2016) (26 observations in Crockett, 51 in Nueces, 18 in Tom Green, 3 in Concho, 2 in Irion) and from our study (9 in Concho, 4 in Tom Green, and 1 in Runnels). From both datasets, a total of 26 presence records have been found in less-developed grasslands and 88 in agricultural areas.

Class proportions in a 10 x 10km grid

Using the land cover datasets at 5-m pixel resolution, we calculated the proportion of each land cover class in a 10 x 10 km grid using ArcGIS Pro. This vector dataset is provided within the Supplementary Data S2. The users of this dataset can then investigate locations with relative proportions of different land cover classes. One of our interests in this analysis was to find areas were agricultural land and grassland-dominated patches are more dominant. As an example, we selected grid cells that have combined significant percentages of grassland-dominated area (more or less than 25%) and more or less of 10% of cropland at the same time (Figure 11). We observed that most of grid cells with combined grassland and cropland occur in the counties of Nueces, Kleberg, Tom Green, Concho, Runnels, and Midland.

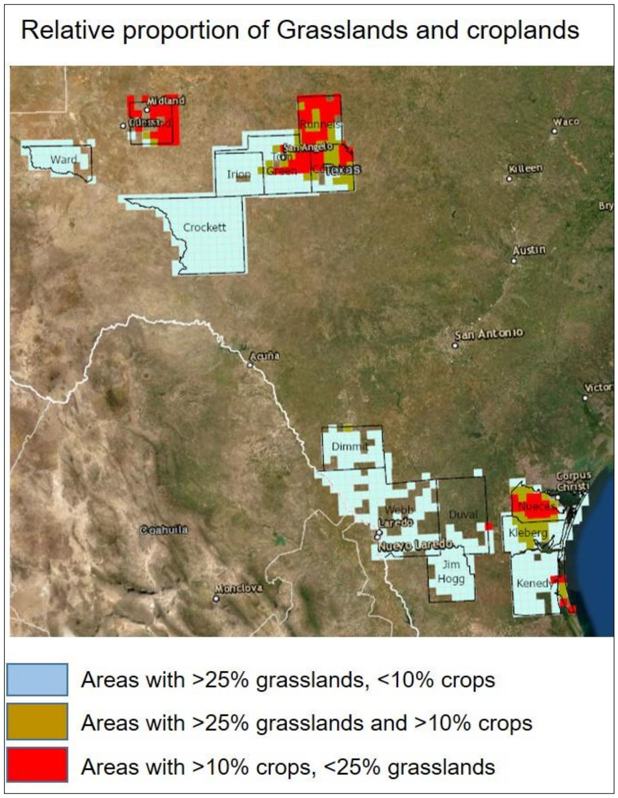

Figure 11. Combined relative proportions of grassland-dominated areas and croplands per grid cell in a 10 x 10 km grid over the study area.

Other products: Percentage of forbs and grasses in grassland-dominated land

We used a new freely available dataset published by the University of Montana (the Rangeland Analysis Platform; https://rangelands.app/). The RAP datasets provide raster datasets of abundance and distribution of perennial or annual herbaceous, shrubs, trees, and bare ground and annual aboveground biomass for the western USA at a 30-m pixel resolution. From this dataset, we combined the “Annual forbs and grasses” and “Perennial forbs and grasses” percentage abundance maps into a single “Annual and perennial forbs and grasses” dataset. This one was subset by the boundaries of grassland-dominated map derived by this project at 0.6 m resolution. By performing this subset, we ensured that RAP observations corresponded to forbs and grass abundance distribution within the available grassland available for STEL. Figure 12 shows the gradient observed of abundance of forbs and grasses across grasslands of the study area. The dataset shows patches of higher abundance of forbs and grasses in north-eastern Crockett, scattered fragments in Concho, Tom Green, and Irion, and in the counties of Jim Hogg, Kleberg, and Kenedy. The RAP data does not discriminate between native and invasive species.

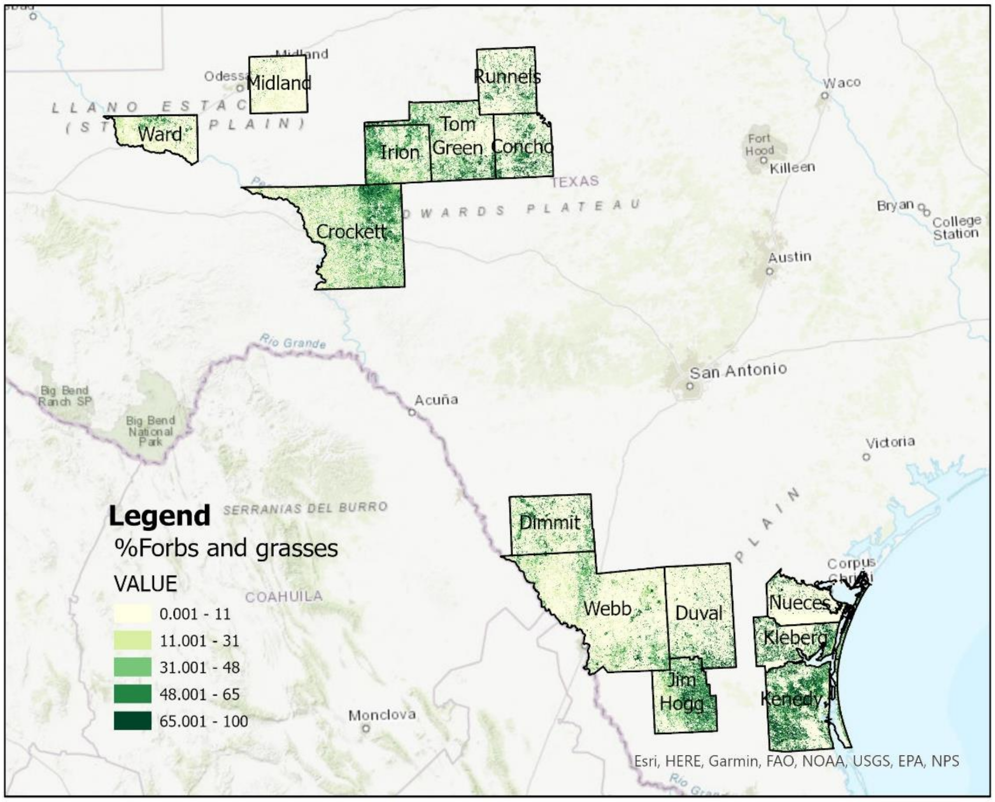

Figure 12. Annual and perennial forbs and grasses abundance within the "Grassland-dominated" class as mapped by this project. The dataset shows patches of higher abundance of forbs and grasses in north-eastern Crockett, scattered fragments in Concho, Tom Green, and Irion, and in the counties of Jim Hogg, Kleberg, and Kenedy. The RAP data does not discriminate between native and invasive species.

Other products: Change in the percentage of forbs and grasses between 1986-2018

Using time series data of tree and shrub abundances from the Rangeland Analysis Platform, we investigated changes in woody plant abundances from 1986 to 2018. The results show that overall abundances were higher for trees and shrubs in 2018 than in 1986 and that an increase in abundance of woody plants has been occurring in most of the counties (Figure 13). Areas with lower change or more stable grasslands can be found in Concho, Ward, Kenedy, Kleberg, and Jim Hogg counties.

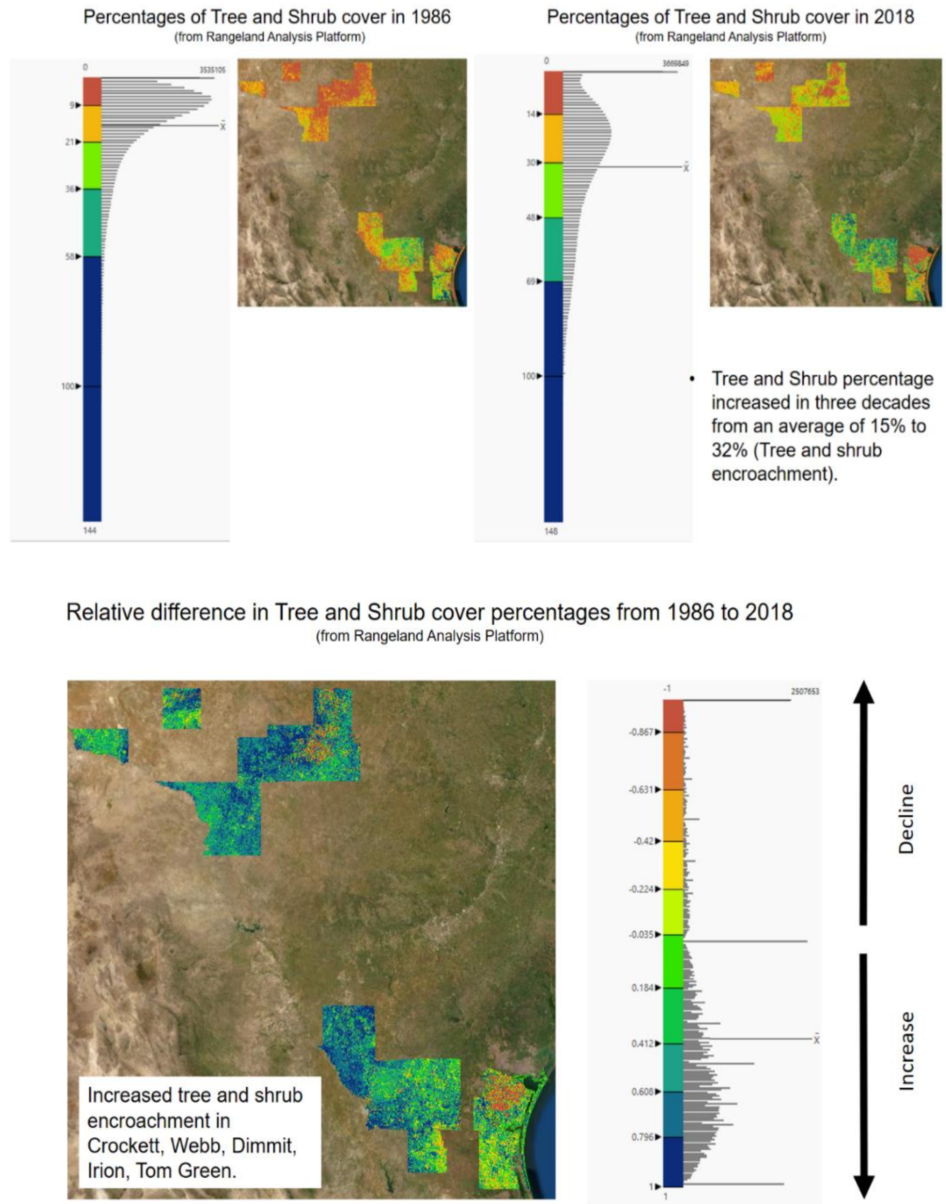

Figure 13. Changes in the distribution of tree and shrub abundance within the 14 counties from 1986 to 2018 as estimated by the Rangeland Analysis Platform products. The dataset shows that overall abundances were higher for trees and shrubs in 2018 than in 1986 and that an increase in abundance of woody plants has been occurring in most of the counties. Areas with lower change or more stable grasslands can be found in Concho, Ward, Kenedy, Kleberg, and Jim Hogg counties.

Other products: habitat selection.

Analysis showed via Wilks lambda test that there was significant ($P < 0.05$) habitat selection (i.e., a difference in land use / land cover types in areas occupied by STEL compared to sites at random). The rankings of habitat show that areas with high % of bare ground and perennial grasses and forbs were selected *for* and trees were selected *against*. This means that presence of STEL was associated with every other land-cover type except trees. In addition, Manly's selection ratios were consistent with previous results, with bare ground, litter, and perennial forbs and grasses having the highest global selectivity ratios (Figure 14). Also, the analysis showed that areas with STEL are more diverse in terms of land-cover types than areas without STEL.

When exploring values of the RAP data within the 200 m buffers, higher percentages of perennial forbs and grasses are found in native grassland areas, as expected. In most cropland pixels, RAP percentage values are close to 0% for all classes, which might reflect the presence of active crops. However, RAP data values show higher percentage litter and percentage bare ground in fallow land. This means that cropland pixels are characterized by near 0% RAP data values in all classes or higher percentages of litter and bare ground. The Manly selectivity ratio results suggest selection for native grasslands, bare ground, and litter (these two as indicators of cropland).

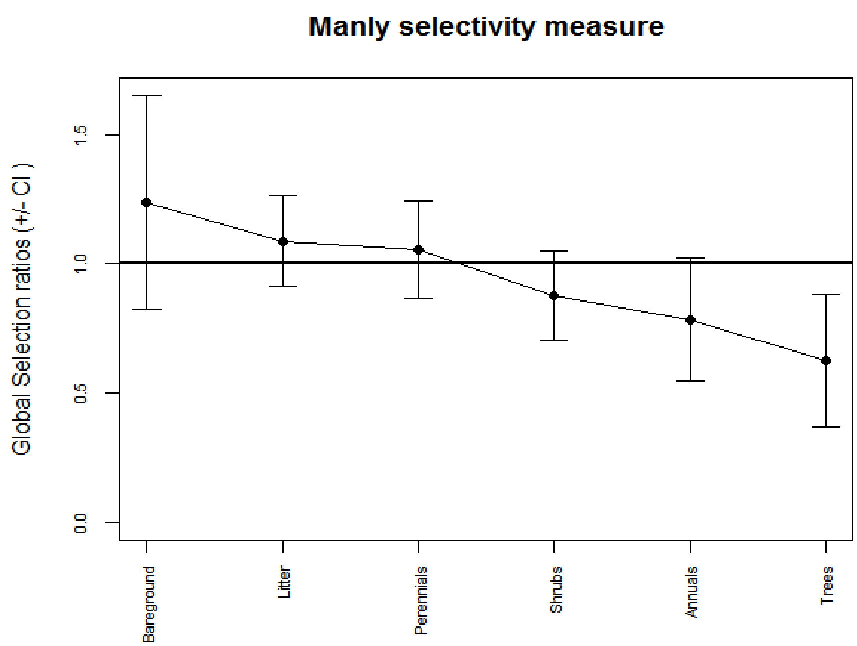

Figure 14. Manly selection ratios for vegetation cover using 49 presence records and 49 random records across Crockett, Irion, Tom Green, Concho, and Runnels counties. Vegetation cover was extracted from the Rangeland Analysis Platform data.

TASK 4. Historical vegetation cover change analysis

Results are shown in Table 4 and Figure 15. As observed in our data, change in vegetation cover in all eight locations (eight counties) was mainly related to increase in vegetation cover due to land abandonment and shrub/tree expansion in grasslands, and decreases in vegetation cover due to urban expansion, land development (industrial and road expansion), and agricultural expansion. Significant decline in vegetation cover was observed in Midland and Runnels counties due to land development and agricultural expansion during the complete time series analysis. The "speed" of change (as depicted by the R value) and magnitude of changes (from changes in area) are varied across space but also across time. In Kenedy and Kleberg counties, agricultural expansion caused a negative trend in vegetation cover after 1996, while Jim Hogg and Nueces have experienced slight increases in cover.

TASK 5. Influence Diagram

Based on field surveys and geospatial products generated in this project, we created an influence diagram based on multiple factors that we consider important in maintaining STEL populations in Texas (Figure 16). Historical records and presence records from this study indicate a prevalence of observations in counties that contain a mix of agricultural land, bare ground (e.g., caliche roads, open grasslands), and native grasslands, and avoidance of areas dominated by woody cover. Indications were confirmed by the habitat selection analysis (Task 3) that showed significant selection of bare ground, native grasses, and cropland-related land covers by STEL.

In the highly developed rural areas of Texas, anthropogenic actions determine the magnitude of these three key factors. Therefore, we consider that the main factor that influences STEL populations in Texas to be land use / land cover change due to human actions. Land cover diversity is a function of native grassland fragmentation due to agricultural, industrial and urban expansion, and road construction, whereas native grassland integrity, the presence of invasive species, and increases in woody cover are controlled by land management (e.g., overgrazing, fire suppression). Dynamics of habitat disturbance and fragmentation due to human population dynamics will determine the availability of STEL habitat across time and the ability of STEL to adapt to new conditions. Understanding the magnitude of land cover diversity and habitat disturbances (invasive species, tree/shrub encroachment) across space and time in Texas will help infer the potential presence of STEL at any point in time, which then will determine land management and conservation decisions.

Table 4. Summary of vegetation cover changes and their main driver of change from 1940's to 2018 for eight 25 km x 25 km grid cells expanding in eight counties.

County	Year	Area_ha	TimeDiff	R (%change/yr)	Main driver of change
JimHogg	**1950**	48462.533	0		
	1995	48166.538	45	-0.000136134	Agricultural expansion
	2018	49012.588	23	0.000757356	Land abandonment
Kenedy	**1943**	43904.853	0		
	1996	48738.428	53	0.001972564	Shrub encroachment
	2018	47385.082	22	-0.001279197	Agricultural expansion
Kleberg	**1950**	11629.441	0		
	1996	18004.199	46	0.009546696	Shrub encroachment
	2018	14425.538	22	-0.010022388	Agricultural expansion
Midland	**1946**	42729.304	0		
	1996	41327.461	50	-0.000666933	Land development
	2018	39135.86	22	-0.002473664	Land development
Nueces	**1938**	5859.9995	0		
	1996	1432.5878	58	-0.023994799	Agricultural expansion
	2018	1563.737	22	0.003989575	Increase in grass patches in developed areas
Runnels	**1940**	19951.628	0		
	1996	15302.826	56	-0.00472582	Agricultural expansion
	2018	12683.53	22	-0.008497024	Agricultural expansion
TomGreen	**1938**	14568.933	0		
	1996	16603.509	58	0.002256381	Shrub encroachment
	2018	13870.084	22	-0.008143017	Urban expansion
Webb	**1952**	48584.214	0		
	1996	48518.262	44	-3.08721E-05	Land development
	2015	45559.677	19	-0.003305956	Land development

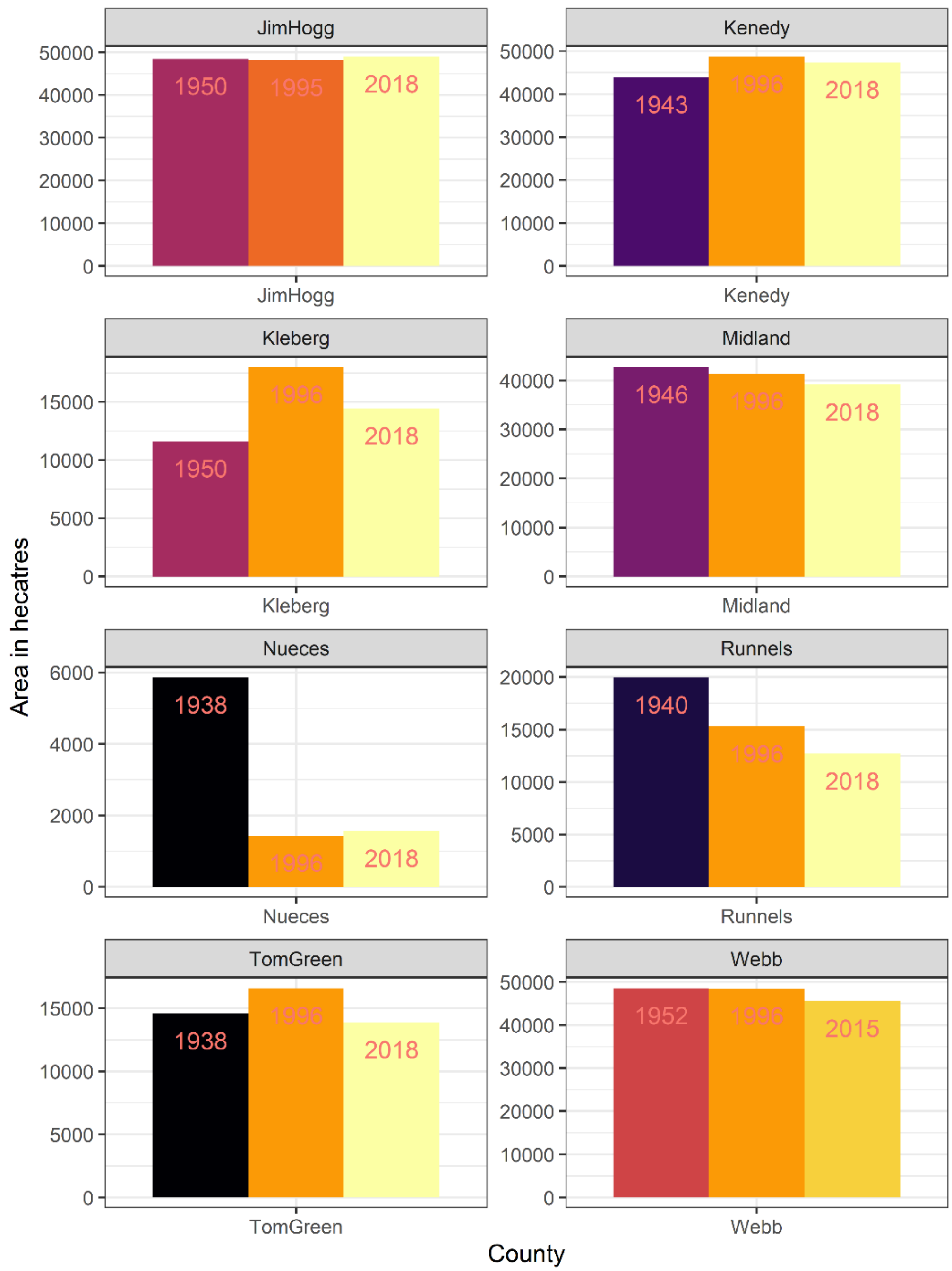

Figure 15. Graph showing the changes of vegetation cover area from 1940's to 2018 for eight 25 km x 25 km grid cells in eight counties.

.

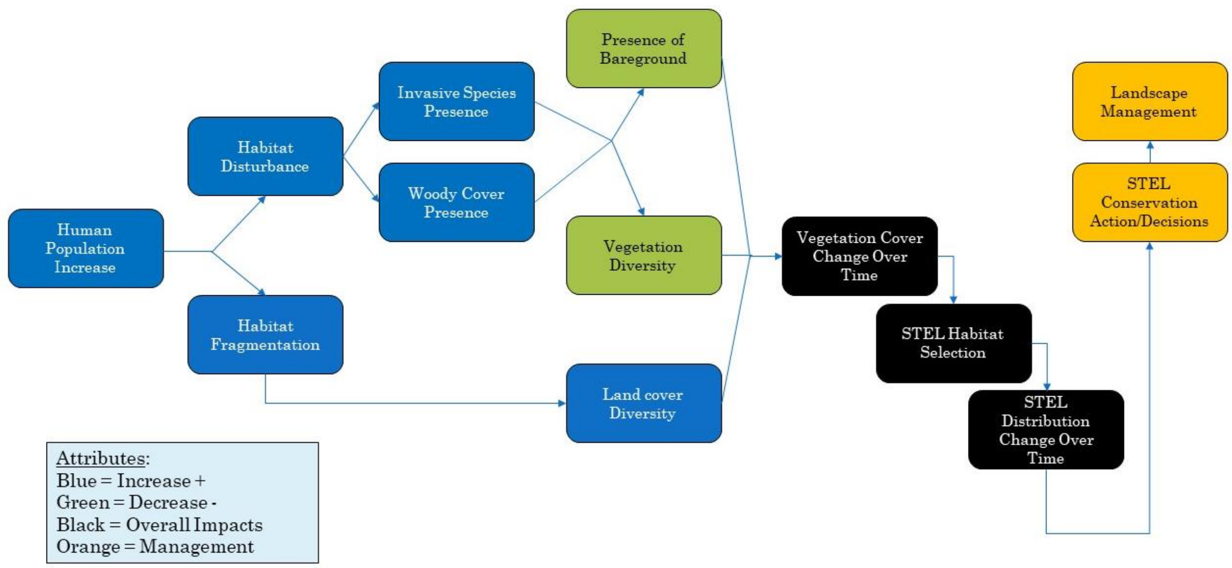

Figure 16. The Influence diagram lists interrelated factors that affect STEL populations in Texas.

DISCUSSION

The objective of our study was to respond to several questions regarding current habitat conditions for STEL. Related questions were grouped into four categories: a) What habitat characteristics are required for STEL? b) Where are the required habitat characteristics found across the landscapes of west and south Texas? Are habitats with suitable characteristics for these species occupied? c) How have habitat characteristics changed over time in the historic range of STEL? d) Does buffelgrass invasion pose a threat to both native Texas species? Does buffelgrass invasion coincide with other land use changes and anthropogenic effects over time?

A) What habitat characteristics are required for STEL?

Both subspecies (now species) of STEL inhabit the historical grasslands of central and Southeast Texas (Axtell, 1954, 1956, 1958). They differ in their respective habitats, the change being delineated by the Balcones Escarpment (Axtell, 1954, 1956, 1958). Both habitats contain sandy to clay loams, not excluding non-clay loams, though never pure sands, over a caliche or limestone base (Axtell, 1954, 1956). The lizard doesn’t appear to have an extreme obligation to very specific habitats, though it does retain a habitat preference orf historic desert grasslands

(Axtell, 1954). However, in general, suitable habitat was determined to be areas that are flat, without pure sands or dense woody encroachment, and with some level of disturbance.

STEL prefers areas that are flat, have less than 3% slope, low woody encroachment, and are sparsely vegetated with bare ground patches (Axtell, 1954, 1958; Duran, 2017; Hibbitts and Ryberg 2017; Duran, 2018). The lizard will seek bare ground when available but also uses areas of dense vegetation (Duran, 2013, 2017). Habitat can be live oak and mesquite savannas, agricultural fields, and coastal prairies garnering some form of disturbance (Axtell, 1954, 1956; Duran, 2013, 2017). Loose soils of agricultural areas may be utilized by the lizard to exploit invertebrates and cover (Axtell, 1956).

During our study, we observed several STEL in overcast, cloudy or scattered thunderstorm weather conditions. Our observations suggest that STEL's temperature threshold for activity may be lower than previously thought. Axtell noted that the southern populations of STEL cease activity at 28 degrees Celsius (Axtell 1956), and Texas A&M biologists, though admitting they are unsure of what effect heavy rains has on lizard activity, stated in their 2018 report "Lizards likely spend more time foraging and consuming prey items early in the season when these prey are more abundant. Conversely, lizard activity slows down as prey become less abundant and as temperatures begin to drop." (Laduc 2018). Thus, the window of opportunity to observe STEL may be larger than currently agreed upon among STEL researchers and is not as influenced by invertebrate activity. If this is true, perhaps STEL has not been observed in historical localities because biologists are limiting opportunistic survey time, and very well be the reason we did not observe the lizard in the Southern counties.

STEL tend to be found in areas surrounded by agricultural land, having heavy anthropogenic influence. Pesticides are a top concern when considering croplands, due to known negative physiological effects on many lizard species (DuRant et al. 2007, Cacki and Akat 2011, Freitas et al. 2020). STEL will use burrows as cover when available and has been observed exhibiting bury behavior (Duran and Yandell 2014, Neuharth et al. 2018). Loose soils in agricultural areas may allow the lizard to avoid predation, and dirt clods and rocks along agricultural roads offer basking/perching locations for STEL The presence of perching areas, loose soils, and basic habitat requirements in agricultural areas may be sufficient for STEL to persist and off-set any negative impacts that the lizard might face.

In general, historical records and presence records from this study confirm STEL habitat requirements. Our results indicate a prevalence of observations in counties that contain a mix of agricultural land, bare ground (caliche roads, open grasslands), and native grasslands, and avoidance of areas dominated by woody cover. This was confirmed by the habitat selection analysis (Task 3) that showed significant selection of bare ground, native grasses, and cropland-related land covers by STEL. Thus, STEL needs habitats that are either disturbed or that remain relatively open by natural processes.

B) Where are the required habitat characteristics found across the landscapes of west and south Texas? Are habitats with suitable characteristics for these species occupied?

Overall patterns

Our results indicated that the grassland-dominated area extends for 1,958,247 hectares (which corresponds to roughly 12,583 square kilometers), which represents 36% of the total study area. The grassland-dominated class had a total core area of 1,498,896 hectares (76% of its extent). Alarmingly, the class was represented by 3,163,341 patches (NP) with a mean area of 1 ha. The grassland-dominated areas therefore occupy roughly a third of the available landscape, although their distribution is highly fragmented and dominated by small (~1 ha) patches.

County-by-county summary

We can summarize our findings in four general patterns as depicted in Figure 8:

A) **Less fragmented grasslands in diverse or heterogeneous landscapes**: Kenedy county has continuous and less fragmented grassland-dominated areas with a balanced proportion of land cover types (i.e., relatively high landscape diversity).
B) **Less fragmented grasslands in homogeneous landscapes**: Jim Hogg county has more continuous grassland-dominated areas in less diverse landscapes.
C) **Fragmented grasslands in heterogeneous landscapes**: Tom Green, Nueces, Concho, Runnels, Midland, and Kleberg counties have fragmented grassland-dominated areas in heterogenous or diverse landscapes.
D) **Fragmented grasslands in homogeneous landscapes**: Duval, Webb, Dimmit, Ward, Irion, and Crockett counties all have fragmented grassland-dominated areas in homogenous and less-diverse landscapes. Crockett seems to occur at the borderline of this group, given its large extensions of grassland at the northeastern edge of the county.

STEL habitat characteristics suggest that heterogenous landscapes with presence of native grasslands (Patterns A and C) will be preferred by STEL. Figure 8 shows that, in fact, most STEL observations have been historically made on counties that fall in Pattern C. However, STEL has not been recorded in Kenedy county (Pattern A) and also, historical records have been found in Crockett and Irion counties, which have significant extensions of native grassland patches and little to no agricultural land.

From historical records, 26 observations have been registered for Crockett, 51 in Nueces, 18 in Tom Green, 3 in Concho, and 2 in Irion. In our study, 9 records were collected in Concho, 4 in Tom Green, and 1 in Runnels. From both datasets, a total of 26 presence records have been found in less-developed grasslands whereas 88 have been found in agricultural areas. This suggests a wide range of conditions at play when determining the current distribution of STEL habitat: STEL can inhabit both native grassland-dominated areas or highly fragmented grasslands within agricultural lands. In both cases, the presence of native grassland patches seems to be essential. Figure 9 shows that continuous high density native grassland only occurs in Crockett, Kenedy, and Jim Hogg counties. The majority of STEL habitat (grassland-dominated land) is highly fragmented, with lower abundances of annual and perennial forbs and grasses within its current extent. The complete loss of these native grasslands may be contributing to STEL population declines (Roelke et al., 2018).

C) How have habitat characteristics changed over time in the historic range of STEL?

Time series analysis of aerial imagery from 1940's to 2018 at specific sample areas indicated that across the study area, the land cover and land use changes observed are complex, without one primary trajectory occurring. The rate of change varied spatially, with agricultural expansion driving change from 1930's to 1990's and then urbanization and industrial development driving land cover and land use changes in the last few decades. Changes in vegetation cover were mainly related to positive changes (increase in vegetation cover) due to land abandonment and shrub/tree expansion in grasslands; negative changes (decreases in vegetation cover) were observed in areas with significant urban expansion, land development (industrial and road expansion), and agricultural expansion. Highest rates of change were registered in Nueces (from 1940's to 1996) and Kleberg (recent, 1996 to 2018) counties, driven by agricultural expansion. Agricultural expansion also had negative impacts on grassland cover in Runnels and Tom Green counties, although these occurred at lower rates of change. Negative changes in Webb and Midland counties were driven by the expansion of roads and rural development.

The analysis of the vegetation cover products from the Rangeland Analysis Platform (RAP) showed interesting results that need to be taken into consideration regarding threats to current STEL habitat. RAP data showed a widespread increase in tree and shrub cover from 1986 to 2018 across STEL habitat. The increase of tree and shrub cover has occurred in all counties but is especially conspicuous in Webb, Dimmit, Crockett, Irion, Tom Green, and Midland. Areas with lower change or more stable grasslands can be found in Concho, Runnels, Ward, Kenedy, Kleberg, and Jim Hogg. Given that woody cover is avoided by STEL, the continued expansion of tree and shrub cover might pose a threat to STEL habitat use in areas where the species is still found today.

D) Does buffelgrass invasion pose a threat to both STEL species? Does buffelgrass invasion coincide with other land use changes and anthropogenic effects over time?

Buffelgrass presence was recorded ain six out of the 14 counties selected for this study. The six counties represent 42% of the territory of potential STEL presence and are located in the southern part of its distribution (Webb, Dimmit, Duval, Nueces, Kenedy, and Kleberg). Buffelgrass was not observed in any of the counties on the northern side of STEL distribution.

Although buffelgrass inhabits warm, frost-free areas, it has been found in northern areas and has the potential to invade northern STEL habitat. The combined threat of buffelgrass invasion and the evidence of increased shrub/tree encroachment in native grasslands have the potential to significantly reduce STEL habitat. We find that buffelgrass presence, as a representative of many other invasive species, is a function of major anthropogenic influence on the landscape, and spreads with increases in human presence and movement over time.

CONCLUSIONS

In this study, the use of high-resolution imagery and field surveys allowed us to document the current conditions of STEL habitat at a finer spatial resolution than any other study to date. Our results indicate that grassland-dominated land occupies roughly a third of the available landscape to STEL, in a distribution that is highly fragmented and consisting primarily of small (~1 ha) patches of grassland. Historical records, our field surveys, and habitat selection analysis indicate that suitable habitat is limited to areas without dense woody vegetation encroachment. Field detections of STEL presence predominantly occurred in counties that contain a mix of agricultural land, bare ground, and native grasslands. We found that STEL can inhabit both native grassland-dominated areas or highly fragmented grasslands with agricultural land. In both cases, the presence of patches of native grassland patches seems to be essential.

Although rates of land cover change have been low and stable in recent decades, and evidence suggest that disturbances such as agricultural expansion and road increase can, in fact, be part of the habitat used by STEL, the combined threat of increased shrub/tree encroachment and buffelgrass invasion in native grasslands has the potential to significantly further reduce STEL habitat in the future.

Future directions

Tracking landscape diversity and native grasslands across STEL distribution is necessary. The evaluation of the composition and condition of native grassland patches within the species' distribution can be performed using a combination of field survey data and remote sensing. Both methods can also be integrated to model the distribution of invasive species at landscape to regional scales. Factors that regulate the expansion of shrubs and trees should also be monitored within STEL habitat.

Our assessment also indicates that future local studies on ecology and behavior of STEL with fine-resolution landscape-level information will improve our understanding of STEL habitat and its resilience in disturbed landscapes. Studies should be focused in areas where STEL has been already found (including agricultural landscapes). Fine-resolution mapping can be derived from imagery collected by Unmanned Aerial Vehicles (UAV) and be used to describe topography, soil characteristics, and vegetation characteristics. Examining whether there are differences in behavior or life-history traits by region would also be fruitful areas for future research.

REFERENCES

Arriaga L., Castellanos V. A. E., Moreno E., Alarcon J. 2004. Potential ecological distribution of alien invasive species and risk assessment: a case study of buffel grass in arid regions of Mexico. Conservation Biology. Vol. 18. pp 1504-1514.

Aronoff, S. (1982). The map accuracy report: a user's view. *Photogrammetric Engineering and Remote Sensing*, *48*(8), 1309–1312.

Axtell, R. 1954. The Systematic Relationships of Certain Lizards in the Genus Holbrookia. Master's thesis. University of Texas.

Axtell, R. 1956. A Solution to the Long Neglected *Holbrookia lacerata* Problem, and the Description of Two New Subspecies of Holbrookia. Bulletin of the Chicago Academy of Sciences 10:11 163–179.

Axtell, R. 1998. *Holbrookia lacerata* Cope. The Interpretive Atlas of Texas Lizards. Self-published.

Baker, B. A., Warner, T. A., Conley, J. F., and McNeil, B. E. (2013). Does spatial resolution matter? A multi-scale comparison of object-based and pixel-based methods for detecting change associated with gas well drilling operations. *International Journal of Remote Sensing*, *34*(5), 1633–1651. https://doi.org/10.1080/01431161.2012.724540

Belgiu, M., and Csillik, O. (2018). Sentinel-2 cropland mapping using pixel-based and object-based time-weighted dynamic time warping analysis. *Remote Sensing of Environment*, *204*(October), 509–523. https://doi.org/10.1016/j.rse.2017.10.005

Blaschke, T. (2010). Object based image analysis for remote sensing. *ISPRS Journal of Photogrammetry and Remote Sensing*, *65*(1), 2–16. https://doi.org/10.1016/j.isprsjprs.2009.06.004

Blaschke, Thomas, Hay, G. J., Kelly, M., Lang, S., Hofmann, P., Addink, E., Queiroz Feitosa, R., van der Meer, F., van der Werff, H., van Coillie, F., and Tiede, D. (2014). Geographic Object-Based Image Analysis - Towards a new paradigm. *ISPRS Journal of Photogrammetry and Remote Sensing*, *87*, 180–191. https://doi.org/10.1016/j.isprsjprs.2013.09.014

Breiman, L. (2001). Random forests. *Machine Learning*, *45*, 5–32. https://doi.org/10.1023/A:1010933404324

Breiman, Leo, Friedman, J. H., Lshen, R. A., and Stone, C. J. (1984). Classification and Regression Trees. In *Chapter 7* (Issue January). Chapman and Hall/CRC.

Cakici, O., and Akat, E. 2012. Histopathological effects of carbaryl on testes of snake-eyed lizard, Ophisops elegans. Environmental Science and Pollution Research 19:1 64–71.

Centre for Arid Zone Research. 2001. Buffel Grass Distribution. Sustainable Ecosystems. CSIRO, Australia.

Cox J. R., Martin-R M. H., Ibarra-F F. A., Fourie J. H., Rethman J. F. G., Wilcox D. G. 1988. The influence of climate and soils on the distribution of four African grasses. Journal of Range Management Vol. 41. pp127-139.

Congalton, R. G. (1991). A review of assessing the accuracy of classifications of remotely sensed data. *Remote Sensing of Environment*, *37*(1), 35–46. https://doi.org/10.1016/0034-4257(91)90048-B

Daehler C. C. and E. M. Goergen 2005. Experimental restoration of an indigenous Hawaiian grassland after invasion by Buffel Grass (Cenchrus ciliaris). Restoration Ecology 13: 380–389.

De la Barrera, E. 2008. Recent invasion of buffel grass (Cenchrus ciliaris) of a natural protected area from the southern Sonoran Desert. Revista Mexicana de Biodiversidad 79:385-392.

Crump, P. S., and M. R. J. Forstner. 2019. Bias and precision of lizard occupancy estimates vary among observers and between methods. Journal of Herpetology 53:1 13–21.

Dahdouh-Guebas, F. (2002). The use of remote sensing and GIS in the sustainable management of tropical coastal ecosystems. In *Environment, Development and Sustainability*. https://doi.org/10.1023/A:1020887204285

Duran, C. M. 2017. An Inventory of a Subset of Historically Known Populations of the spot-tailed earless lizard (*H. lacerata*).

Duran C.M., and Axtell R.W. 2011. The status of and a predictive habitat model for H. lacerata (the spot-tailed earless lizard): Response to a request for information from the Department of the Interior, US Fish and Wildlife Service.

Duran, C. M., and D. L. Yandell. 2014. H. lacerata subcaudalis (Southern Spot-tailed Earless Lizard) Refugia and Commensalism. Herpetological Review 45:501–502.

DuRant, S.E., Hopkins, W.A., and Talent, L.G. 2007. Energy acquisition and allocation in an ectothermic predator exposed to a common environmental stressor. Comparative Biochemistry and Physiology 145:3 442–448.

Elliott, L. F., Diamond, D. D., True, C. D., Blodgett, C. F., Pursell, D., German, D., and Treuer-Kuehn, A. (2014). *Ecological Mapping Systems of Texas: Summary Report*. *April*.

Franklin, S.E., Wulder, M. A., and Gerylo, G. R. (2001). Texture analysis of IKONOS panchromatic data for Douglas-fir forest age class separability in British Columbia. *International Journal of Remote Sensing*, *22*(13), 2627–2632.

Freitas, L.M., Paranaíba, J.F.F.S, Peréz, A.P.S., Machado, M.R.F., and Lima, F.C. 2020. Toxicity of pesticides in lizards. Human and Experimental Toxicology 39:5 596–604.

Fry, J. A., Coan, M. J., Homer, C. G., Meyer, D. K., and Wickham, J. D. (2009). Completion of the National Land Cover Database (NLCD) 1992 – 2001 Land Cover Change Retrofit Product. In *U.S. Geological Survey Open-File Report*. https://doi.org/10.1608/FRJ-3.1.2

Giocomo, J., J. Hayes, K. Gee, J. Raasch, and R. Perez. 2017. Strategic habitat conservation for declining grassland wildlife populations in the Oaks and Prairies Joint Venture. National Quail Symposium Proceedings 8:57-64.

Grice A. C. 2006. The impact of invasive plant species on the biodiversity of Australian rangelands. The Rangeland Journal. Vol. 28. pp 27-35.

Hanselka C.W. 1988. Buffelgrass: South Texas wonder grass. Rangelands Vol. 10, No. 6. pp 279-281.

Hesselbarth, M.H.K., Sciaini, M., With, K.A., Wiegand, K. and Nowosad, J. (2019), *landscapemetrics*: an open-source *R* tool to calculate landscape metrics. Ecography, 42: 1648-1657. https://doi.org/10.1111/ecog.04617

Hayes, M. M., Miller, S. N., and Murphy, M. A. (2014). High-resolution landcover classification using random forest. *Remote Sensing Letters*, *5*(2), 112–121. https://doi.org/10.1080/2150704X.2014.882526

Homer, C. G., Dewitz, J. A., Yang, L., Jin, S., Danielson, P., Xian, G., Coulston, J., Herold, N. D., Wickham, J. D., and Megown, K. (2011). Completion of the 2006 National Land Cover Database for the conterminous United States. *Photogrammetric Engineering and Remote Sensing*. https://doi.org/citeulike-article-id:4035881

Homer, C. G., Dewitz, J. A., Yang, L., Jin, S., Danielson, P., Xian, G., Coulston, J., Herold, N. D., Wickham, J. D., and Megown, K. (2015). Completion of the 2011 National Land Cover Database for the conterminous United States-Representing a decade of land cover change information. *Photogrammetric Engineering and Remote Sensing*, *81*(5), 345–354. https://doi.org/10.14358/PERS.81.5.345

Ingram, M. 2017. The endangered species act in Texas: A survey and history. Texas Public Policy Foundation publication.

Jackson J. 2005. Is there a relationship between herbaceous species richness and buffel grass (Cenchrus ciliaris)? Austral Ecology 30:505-517.

Knight, J. F., Tolcser, B. P., Corcoran, J. M., and Rampi, L. P. (2013). The effects of data selection and thematic detail on the accuracy of high spatial resolution wetland classifications. *Photogrammetric Engineering and Remote Sensing*, *79*(7), 613–623. https://doi.org/10.14358/PERS.79.7.613

Kuhn, M. (2020). *caret: Classification and Regression Training*. https://cran.r-project.org/package=caret

Kuvlesky, W. P., T. E. Fulbright, R. Engel-Wilson. 2002. The impact of invasive exotic grasses on quail in the Southwestern United States. National Quail Symposium Proceedings 5: 118-128.

LaDuc, T. J., B. D. Wolaver, J. P. Pierre, C. M. Duran, B. J. Labay, W. A. Ryberg, C. E. Roelke, M. K. Fujita, I. M. Wright, G. Surya, C. J. Shank, P. Holloway, R. J. Andrews, S. A. Ikonnikova, and G. McDaid. 2018. Final Report: Collaborative research on the natural history of the enigmatic spot-tailed earless lizard (Holbrookia lacerata) in Texas. Prepared for the Texas Comptroler of Publica Accounts May 7, 2018.

Lopez, R. 2018. Texas Land Trends Presentation: How and Why Texas is Changing. Texas A&M Natural Resources Institute, Texas A&M Agrilife Research Extension.

Li, X., and Shao, G. (2014). Object-based land-cover mapping with high resolution aerial photography at a county scale in midwestern USA. *Remote Sensing*, *6*(11), 11372–11390. https://doi.org/10.3390/rs61111372

Liaw, A., and Wiener, M. (2002). Classification and Regression by randomForest. *R News*.

Liu, T., and Yang, X. (2015). Monitoring land changes in an urban area using satellite imagery, GIS and landscape metrics. *Applied Geography*. https://doi.org/10.1016/j.apgeog.2014.10.002

Mafanya, M., Tsele, P., Botai, J., Manyama, P., Swart, B., and Monate, T. (2017). Evaluating pixel and object based image classification techniques for mapping plant invasions from UAV derived aerial imagery: Harrisia pomanensis as a case study. *ISPRS Journal of Photogrammetry and Remote Sensing*, *129*, 1–11. https://doi.org/10.1016/j.isprsjprs.2017.04.009

Maxwell, Aaron E., Strager, M. P., Warner, T. A., Ramezan, C. A., Morgan, A. N., and Pauley, C. E. (2019). Large-area, high spatial resolution land cover mapping using random forests, GEOBIA, and NAIP orthophotography: Findings and recommendations. *Remote Sensing*, *11*(12). https://doi.org/10.3390/rs11121409

Myint, S. W., Gober, P., Brazel, A., Grossman-Clarke, S., and Weng, Q. (2011). Per-pixel vs. object-based classification of urban land cover extraction using high spatial resolution imagery. *Remote Sensing of Environment*, *115*(5), 1145–1161.

https://doi.org/10.1016/j.rse.2010.12.017

Nagel, P., and Yuan, F. (2016). High-resolution land cover and impervious surface classifications in the twin cities metropolitan area with NAIP Imagery. *Photogrammetric Engineering and Remote Sensing*, *82*(1), 63–71. https://doi.org/10.14358/PERS.83.1.63

NatureServe Explorer. 2019. Comprehensive species report – H. lacerata . <http://explorer.natureserve.org/servlet/NatureServe?searchName= Holbrookia+lacerata>. Accessed May 2019.

Pauchard A., Shea K. 2006. Integrating the study of non-native plant invasions across spatial scales. Biological Invasions Vol. 8. pp 399-413.

Piggot J. P. 1995. The weed status of buffel grass (Cenchrus ciliaris L.) and its threat to nature conservation in Western Australia. Unpublished report, Department of Conservation and Land Management, Perth.

Pontius, R. G., and Parmentier, B. (2014). Recommendations for using the relative operating characteristic (ROC). *Landscape Ecology*, *29*(3), 367–382. https://doi.org/10.1007/s10980-013-9984-8

R Core Team. (2020). *R: A language and environment for statistical computing* (4.0.0). R Foundation for Statistical Computing. https://www.r-project.org/

Skidmore, A. K., Bijker, W., Schmidt, K., and Kumar, L. (1997). Use of remote sensing and GIS for sustainable land management. *ITC Journal*.

Stevens, J. M., and J. S. Fehmi 2009. Competitive effect of two nonnative grasses on a native grass in southern Arizona. Invasive Plant Science and Management 2:379-385

Stohlgren, T. J., C. Jarnevich, G. W. Chong, and P. H. Evangelista. 2006. Scale and plant invasions: a theory of biotic acceptance. Preslia 78:405-426.

Texas Parks and Wildlife Department (TPWD). 2013. The TXNDD Report, Data Highlight: Spot-tailed Earless Lizard (Holbrookia lacerta). The Texas Natural Diversity Database, Wildlife Diversity Program, Texas Parks and Wildlife Dept.

Tilman, D., and C. Lehman. 2001. Human-caused environmental change: impacts on plant diversity and evolution. Proceedings of the National Academy of Sciences of the United States of America 98:5433-5440.

Trimble. (2020). *eCognition Developer 9;Sunnyvale, CA, USA*.

Tsendbazar, N. E., Herold, M., de Bruin, S., Lesiv, M., Fritz, S., Van De Kerchove, R., Buchhorn, M., Duerauer, M., Szantoi, Z., and Pekel, J. F. (2018). Developing and applying a multi-purpose land cover validation dataset for Africa. *Remote Sensing of Environment*, *219*(October), 298–309. https://doi.org/10.1016/j.rse.2018.10.025

United States Department of Agriculture. Natural Resources Conservation Services. 2019. Pennisetum ciliare (L.) Buffelgrass. Plants Profile. (online) Retrieved from https://plants.usda.gov/core/profile?symbol=PECI. Accessed July 2019.

United States Fish and Wildlife Service (USFWS). 2011a. Endangered Species Recovery Program. Endangered Species Program, Arlington, VA, USA.

United States Fish and Wildlife Service (USFWS). 2011b. Endangered and Threatened Wildlife and Plants; 90-day finding on a petition to list the Spot-tailed earless lizard as Endangered or Threatened. Department of the Interior, Fish and Wildlife Service. Docket No. FWS-R2-ES-0017; MO 92210-0-0008B2. Federal Register v76.

Wild Earth Guardians. 2010. Petition to list the Spot-tailed earless lizard (Holbrookia lacerta) under the U.S. Endangered Species Act. http://www.wildearthguardians.org/legal/listing_petition_lizard_1.13.10.pdf. Accessed 18 June 2018.

Williams, D. G., and Z. Baruch 2000. African grass invasion in the Americas: ecosystem consequences and the role of ecophysiology. Biological Invasions 2:123-140.

Wolaver, B. D., Pierre, J.P., Labay, B.J., LaDuc, T.J., Duran, C.M., Ryberg, W.A., and Hibbitts, T.J. 2018. An approach for evaluating changes in land-use from energy sprawl and other anthropogenic activities with implications for biotic resource management. Environmental Earth Sciences 77:5 1–14.

Yu, Q., Gong, P., Clinton, N., Biging, G., Kelly, M., and Schirokauer, D. (2006). Object-based detailed vegetation classification with airborne high spatial resolution remote sensing imagery. *Photogrammetric Engineering and Remote Sensing*, *72*(7), 799–811. https://doi.org/10.14358/PERS.72.7.799

Zurqani, H. A., Post, C. J., Mikhailova, E. A., Cope, M. P., Allen, J. S., and Lytle, B. A. (2020). Evaluating the integrity of forested riparian buffers over a large area using LiDAR data and Google Earth Engine. *Scientific Reports*, 1–16. https://doi.org/10.1038/s41598-020-69743-z